NISTIR 3980

OXIDES AND OXIDE SUPERCONDUCTORS: ELASTIC AND RELATED PROPERTIES

Ming Lei
Hassel Ledbetter

United States Department of Commerce
National Institute of Standards and Technology

NISTIR 3980

OXIDES AND OXIDE SUPERCONDUCTORS: ELASTIC AND RELATED PROPERTIES

Ming Lei[†]
Hassel Ledbetter

Materials Reliability Division
Materials Science and Engineering Laboratory
National Institute of Standards and Technology
Boulder, Colorado 80303-3328

August 1991

[†]Visiting Scientist, on leave from the Institute of
Metal Research, Academia Sinica, Shenyang, China

U.S. DEPARTMENT OF COMMERCE, Robert A. Mosbacher, Secretary
NATIONAL INSTITUTE OF STANDARDS AND TECHNOLOGY, John W. Lyons, Director

Contents

List of Tables

List of Figures

Abstract

Using both measurements and modeling, we studied the elastic and related properties of some oxides and oxide superconductors. The polycrystal elastic constants were measured using a megahertz-frequency pulse-echo method between 295 and 4 K and corrected to the void-free state by using a model for a composite material containing spherical particles. The elastic moduli of the high-T_c superconductor $Y_1Ba_2Cu_3O_7$ (YBCO) were compared with that of oxides, especially the perovskites $BaTiO_3$ and $SrTiO_3$, which are crystal-structure building blocks for the YBCO superconductor. The bulk moduli were also calculated using a Born ionic model with two energy terms: electrostatic (Madelung) and ion-core-repulsion. The calculated bulk modulus of YBCO, 98 GPa, agrees well with measurement, 101 GPa. Based on monocrystal measurements combined with analysis–theory, elastic stiffnesses C_{ij} for orthorhombic YBCO were estimated. The bulk modulus obtained from the estimated C_{ij} by the Voigt—Reuss—Hill averaging method agrees with the monocrystal measurement. From the measured polycrystal elastic constants, the Debye characteristic temperatures, Θ_D, were calculated. For YBCO, $\Theta_D^0 = 437$ K. The electron—phonon parameters, λ, were estimated from T_c and Θ_D^0 using Kresin's model, which is valid for all values of λ. For YBCO, $\lambda = 2.24$. Calculating the Madelung energy allowed us to study two further features: the valence of copper and the electron hole distribution. The results show that the hole prefers the CuO_2 plane at the oxygen sites. All the results are consistent with the assumption that all copper ions have valences near +2. Using a relationship between T_c and ΔV_A, the difference in Madelung site potentials for a hole at the apical and planar oxygens, the pressure derivative and stress and stain derivatives of T_c were calculated. The results show that T_c increases with decreasing a-axis, increasing b-axis, and decreasing c-axis.

Key words: Born model; bulk modulus; Debye temperature; elastic constants; electron–phonon parameter; Kresin model; oxides; pressure derivative; superconductors; $Y_1Ba_2Cu_3O_7$.

Chapter 1

Introduction

1.1 Elastic Constants

A material's elastic properties are important because they relate to various fundamental solid-state phenomena [1]. These phenomena include interatomic potentials, equations of state, phonon spectra, and so on. Elastic properties also link thermodynamically with specific heat, thermal expansivity, Debye temperature, and Grüneisen parameter. In engineering design, elastic constants enter many practical applications: load-deflection, thermoelastic stress, internal strain (residual stress), sound velocities, and fracture toughness.

Elastic constants appear in the generalized Hooke's law:

$$\sigma_{ij} = C_{ijkl}\varepsilon_{kl}. \tag{1.1}$$

Here, σ_{ij} and ε_{kl} denote the second-rank stress tensor and strain tensor, respectively; C_{ijkl} indicates components of a fourth-rank elastic-constant tensor; and the usual summation convention is applied to repeated indices. The elastic constants C_{ijkl} can be calculated from a solid's internal energy U [2]:

$$C_{ijkl} = \frac{1}{V_a}\left(\frac{\partial^2 U}{\partial\eta_{ij}\partial\eta_{kl}}\right). \tag{1.2}$$

Here, η_{ij} denotes components of the Lagrangean elastic-strain matrix, and V_a denotes atomic volume. By invoking the Voigt contraction convention,

the fourth-rank-tensor elastic constants can be arranged in a symmetrical six-by-six matrix:

$$C_{ij} = \begin{pmatrix} C_{11} & C_{12} & C_{13} & C_{14} & C_{15} & C_{16} \\ & C_{22} & C_{23} & C_{24} & C_{25} & C_{26} \\ & & C_{33} & C_{34} & C_{35} & C_{36} \\ & & & C_{44} & C_{45} & C_{46} \\ & & & & C_{55} & C_{56} \\ & & & & & C_{66} \end{pmatrix}. \tag{1.3}$$

The generalized Hooke's law can also be expressed in the following way:

$$\varepsilon_{ij} = S_{ijkl}\sigma_{kl}. \tag{1.4}$$

Here, S_{ijkl} denotes components of a fourth-rank elastic-compliance tensor. Similarly, the elastic-compliance tensor S_{ijkl} can also be arranged in a symmetrical six-by-six matrix. Generally, there is a simple relationship between elastic stiffnesses C_{ij} and elastic compliances S_{ij}:

$$[S_{ij}] = [C_{ij}]^{-1}. \tag{1.5}$$

In the most general case (triclinic symmetry), there are twenty-one independent elastic constants. The number of independent elastic constants is reduced by the crystal-class symmetry operations. For example, when a material possesses orthorhombic symmetry there are only nine independent elastic constants; a cubic crystal possesses three. For an isotropic material, there are only two independent elastic constants: C_{11}^0 and C_{12}^0. In engineering usage, there are four practical elastic constants:

$$Shear\ modulus = G = \frac{1}{2}(C_{11}^0 - C_{12}^0), \tag{1.6}$$

$$Young\ modulus = E = \frac{(C_{11}^0 - C_{12}^0)(C_{11}^0 + 2C_{12}^0)}{C_{11}^0 + C_{12}^0}, \tag{1.7}$$

$$Bulk\ modulus = B = \frac{GE}{3(3G - E)} = \frac{1}{3}(C_{11}^0 + 2C_{12}^0), \tag{1.8}$$

$$Poisson\ ratio = \nu = \frac{E}{2G} - 1 = \frac{C_{12}^0}{C_{11}^0 + C_{12}^0}. \tag{1.9}$$

These four elastic constants have particular physical meanings. For example, the bulk modulus describes a solid's resistance to volume change; Young and shear moduli describe a solid's resistance to extensional strain and shear strain, respectively; and the Poisson ratio represents a dimensionless ratio of elastic constants that, for uniaxial stress, relates longitudinal and transverse strains.

1.2 Superconductivity and Elastic Constants

In 1911, Kamerlingh-Onnes [3] found that the electrical resistance of mercury vanished when the temperature dropped to 4 K. The phenomenon that materials lose their resistances when temperature is below a critical value T_c is called superconductivity. When the temperature exceeds T_c, materials have resistances typifying the normal state. The transition between normal and superconducting states is a second-order phase transition, which is characteristic of order–disorder transitions. In a magnetic field, a superconductor can stay in the normal state even though the temperature is below T_c. The minimum magnetic field that destroys superconductivity is called the critical field H_c. Similarly, the minimum current density that destroys superconductivity is called the critical-current density J_c.

For practical use of superconductivity, scientists are trying to raise these three critical parameters, especially the critical transition temperature T_c, as far as possible. Meanwhile, theorists try to link T_c to fundamental physical properties. In 1957, Bardeen, Cooper, and Schrieffer [4] proposed a microscopic theory of superconductivity based on the interaction between electrons and phonons. They gave a simple relationship that relates T_c to the Debye temperature Θ_D:

$$T_c = 1.14\Theta_D \exp(-1/\lambda). \tag{1.10}$$

Here, λ denotes the electron–phonon coupling parameter, which also depends on Θ_D.

On the other hand, the Debye temperature Θ_D can be calculated from the following relationship [5]:

$$\Theta_D = \frac{h}{k}\left(\frac{3N}{4\pi V}\right)^{1/3} v_m. \tag{1.11}$$

Here, h and k denote the Planck and Boltzmann constants, respectively; N denotes the number of independent three-dimensional oscillators in a volume V; and v_m denotes mean sound velocity calculated by the relationship

$$v_m^{-3} = \frac{1}{3}\left(v_\ell^{-3} + 2v_t^{-3}\right). \tag{1.12}$$

Here, v_ℓ and v_t denote longitudinal and transverse velocities, respectively.

The electron–phonon parameter λ is defined by [6]:

$$\lambda = 2\int \frac{\alpha^2 F(\omega)}{\omega} d\omega. \tag{1.13}$$

Here, $\alpha^2 F(\omega)$ represents the Eliashberg electron–phonon coupling function, where $F(\omega)$ indicates phonon density-of-states. By assuming a Debye phonon distribution, $F(\omega) \sim \omega^2$, and taking α^2 to be frequency independent, we find that

$$\lambda = \frac{3\alpha^2 V_a \omega_D^2}{2\pi^2 v_m^3}, \tag{1.14}$$

where

$$\omega_D = \frac{k}{\hbar}\Theta_D \tag{1.15}$$

is the Debye cut-off frequency. Substituting Eqs. (1.15) and (1.11) into Eq. (1.14), we obtain

$$\lambda = \frac{6\alpha^2}{v_m}\left(\frac{3V_a^{1/2}}{4\pi}\right)^{2/3}. \tag{1.16}$$

Equations. (1.10), (1.11), and (1.16) show how the superconducting transition temperature T_c depends on the elastic constants explicitly through both Θ_D and λ.

1.3 Purposes of the Study

The present research focused on the elastic constants of high-T_c metal-oxide superconductors, mainly $Y_1Ba_2Cu_3O_7$ (henceforth written YBCO). This study had nine objectives:

1. Determine the ambient-temperature intrinsic elastic constants of YBCO.

2. Determine the temperature dependence of the YBCO elastic constants in the 295–4 K temperature range.

3. Determine the temperature-dependent elastic constants of $BaTiO_3$ and $SrTiO_3$.

4. Compare YBCO with other oxides, especially the perovskites $BaTiO_3$ and $SrTiO_3$, which are crystal-structure building blocks for the YBCO metal-oxide superconductor.

5. Calculate the bulk modulus of YBCO using a Born ionic model.

6. Estimate the nine independent elastic constants C_{ij} for orthorhombic YBCO using measurements on monocrystals combined with some analysis–theory.

7. Estimate some related physical parameters such as the Debye characteristic temperature Θ_D and the electron–phonon interaction parameter λ.

8. Consider the valence problem, for both the cations (Y, Ba, Cu) and the anion (O). Especially, focus on Cu, which has two site symmetries, thus two possible valences.

9. Estimate the stress dependence of the normal–superconducting transition temperature, $dT_c/d\sigma_{ij}$.

Chapter 2

Previous Elastic-constant Studies

In this chapter, studies of elastic and related properties on high-T_c oxide superconductors, especially YBCO, will be reviewed briefly. Since the crystal structure of YBCO consists approximately of three stacked perovskite unit cells, the review will also include the studies on $BaTiO_3$ and $SrTiO_3$, two representative perovskites.

2.1 Perovskites

2.1.1 $BaTiO_3$

Since barium titanate is a displacive-type ferroelectric, most researches on elastic constants of barium-titanate were combined with studies on dielectric and piezoelectric properties. In 1951, using an ultrasonic pulse method, Bond, Mason, and McSkimin [7] first measured the elastic and dielectric constants of monocrystal barium titanate. For elastic constants and compliances, they reported only S_{11}, $2S_{12}+S_{66}$, and C_{33}. In 1956, Bechmann [8] measured the complete elastic constants for transversely isotropic barium-titanate ceramics (an electric field was applied to the isotropic ceramics). A complete set of elastic, piezoelectric, and dielectric constants of monocrystal barium titanate was given by Berlincourt and Jaffe [9]. They reported the elastic constants of both tetragonal (at 25°C) and cubic (at 150°C) crystal struc-

tures. Using relationships derived by Voigt, Berlincourt and Jaffe calculated the elastic constants of polycrystals from the monocrystal measurements. They found good agreement with Bechmann's [8] results.

The temperature dependence of elastic properties of $BaTiO_3$ was studied by many researchers [9–17]. However, most of the studies focused on high temperature, around 120°C (the Curie point). Only a few authors extended the studies to low temperature, and all of the studies were within the temperature range of −50 to 190°C. Berlincourt and Jaffe [9] and Huibregtse and coworkers [10] observed a large temperature dependence of the elastic compliances of $BaTiO_3$ near the Curie point. Using a composite-bar method, Fushimi and Ikeda [11] found a larger temperature dependence than [9, 10] near the Curie point. They concluded the difference may arise from electrical bias. The temperature dependences of the elastic moduli C_{11} and E were measured by Strukov and Garland [12] and by Mader and coworkers [13], respectively. Singularities of the elastic properties of $BaTiO_3$ caused by structural changes near the tetragonal–cubic phase transition were reported by Perro and Fritsberg [14]. Also, the higher-order elastic constants were studied [15, 16]. Against expectation, Beige and Schmidt [15] found that third-order elastic compliances depend more on temperature than do the second-order. This suggests strong anharmonic effects.

Unlike the measurements, only a few model calculations of elastic properties of $BaTiO_3$ have been done [18–22]. Using a method of power expansion of free energy, Devonshire [18] derived a complete set of elastic, dielectric, and piezoelectric constants from the measurements of Bond and coworkers [7]. Devonshire's elastic constants show the type of anisotropy found later by measurements [9], but to a larger degree. The reason might be that his model fails to consider geometric changes at the Curie point [9]. Turik [19] proposed a general calculational method and derived equations for determining the physical constants of a monocrystal with a 90° laminar structure using known values of the constants of a monodomain tetragonal crystal. Yokoyama, Pak, and Kinase [20] calculated the elastic compliances of $BaTiO_3$ by using a point-dipole model, which considers the dipole–dipole interactions and interatomic forces of the type r^{-m} (m =6, 9). Their model calculation agrees with observation in the ferroelectric phase, but departs from measurements on the paraelectric phase [10]. Beige [21] developed a thermodynamic model that predicts the temperature behavior of second-order and third-order elastic, dielectric, and electromechanical coefficients

for a first-order phase transition. For paraelectric $BaTiO_3$, Beige concluded that the polar defects produce a linear coupling between the order parameter and the mechanical stress.

2.1.2 $SrTiO_3$

Although $SrTiO_3$ and $BaTiO_3$ possess the same crystal structure, they show different dynamical behavior. $BaTiO_3$'s Curie temperature (400 K) is associated with the softening of the lower-zone-center transverse optic mode [22]. $SrTiO_3$ undergoes an antidistortive transition at 110 K associated with the lowering of a zone-boundary optical frequency [22]. $SrTiO_3$ has attracted increasing attention from different branches of solid-state physics. A principal reason for the interest in this material is that its structural transition is associated with condensation of a lattice mode, often referred to as a soft mode [23]. Previous studies on elastic properties of $SrTiO_3$ include both measurements [15,24–39] and calculations [34,37–40].

Among the measurements, Poindexter and Giardini [24] measured elastic compliances S_{ij} for cubic $SrTiO_3$ specimens by using a resonance method. Also for cubic $SrTiO_3$, Bell and Rupprecht [25] and Wachtman and coworkers [26] measured elastic stiffnesses C_{ij} using a pulse-echo method and both found results in good agreement with those of Poindexter and Giardini except C_{11}. The temperature dependence of the elastic properties of $SrTiO_3$ was studied extensively [15,25,27,28,30,31,34–37]. All the studies confirmed that a phase transition occurs near 110 K in $SrTiO_3$. But the phase transition at 36 K reported by Sorge and Hegenbarth [28] remains to be verified. Using a pulse-echo method, Rehwald [35] measured various elastic stiffnesses and compliances in the 130–4 K temperature range, but failed to find any evidence that might indicate a phase transition near 40 K. Höchli and Bruce [37] measured the elastic compliance S_{11} in the temperature region 60−125 K using a resonance method. Near the phase-transition temperature, they observed a stronger singularity than that suggested by earlier measurements [31,34,36] that used pulse-echo techniques. They think that their results indicate a dynamic defect-controlled central-peak phenomenon. Higher-order elastic stiffnesses [29,30,32,33,38,39] and compliances [15] were also studied.

Only a few calculations on $SrTiO_3$ were reported. Using a rigid-shell model with Coulomb and short-range central-force interaction, Achar,

Barsch, and Cross [38,39] calculated the third-order elastic constants of both $SrTiO_3$ and $BaTiO_3$. The $SrTiO_3$ results show that the model gives a consistent description of third-order elastic constants.

2.2 YBCO Superconductor

In 1964, Schooley and coworkers [41] first reported superconductivity in $SrTiO_3$, an oxide with perovskite crystal structure, with a quite low transition temperature, $T_c = 0.3$ K. In 1975, Sleight and coworkers [42] found a higher superconducting transition temperature at 13 K in $BaPb_{1-x}Bi_xO_3$. In 1986, Bednorz and Müller [43] reported a remarkable superconducting transition at 30 K in $La_{1.85}Ba_{0.15}CuO_3$ (LBCO). Almost one year later, Wu and colleagues [44] reported superconductivity in $Y_1Ba_2Cu_3O_7$ (YBCO), with $T_c = 90$ K. Since then, there appeared many studies on the elastic constants, and related properties, of YBCO. Several review papers on this subject exist [45–50].

The studies on the elastic and related properties of YBCO can be divided as follows: room-temperature sound velocities and elastic moduli [51–53,70–72,76–91]; temperature dependence of sound velocities and elastic moduli [53–79,92–138]; temperature dependence of internal friction and attenuation [55–62,73,93–108,139–158]; Debye temperature [51,54,62,68–70,78,83,86,95,120,159–164]; linear thermal expansivity [62,68,69,79,85,95,120,166]; specific heat [73, 95, 159, 162–165]; temperature dependence of ultrasonic frequency [59, 76, 106, 139, 143, 145–149, 167–169]. Among these studies, only thirteen papers reported the single-crystal properties of YBCO [93,109–115,169–173].

Block and coworkers [52] measured the room-temperature bulk modulus using a high-pressure X-ray-diffraction method and obtained $B = 196 \pm 17$ GPa. Using a similar method, Dietrich and coworkers [80] found $B = 170$ GPa and Fietz and coworkers [81] obtained 180 GPa; but Jaya [82] reported a very different result, $B = 92.9$ GPa. Glazkov and coworkers [89] applied neutron diffraction to study the compressibility κ of YBCO at high pressure. For the orthorhombic phase, they obtained $\kappa \approx 5.7 \times 10^{-3}$ GPa^{-1}, that is, the bulk modulus $B = 175.4$ GPa. Using an ultrasonic pulse-echo method, Ledbetter and coworkers [51] found a much lower value of B, 72 GPa, corrected to the void-free state. Also by measuring ultrasonic wave velocities, Al-Kheffaji and coworkers [83] and Cankurtaran and coworkers [84] reported

that $B = 68.5$ GPa for the nonporous YBCO. Some authors reported an even lower value for the bulk modulus, for example, 46.3 GPa (at 205 K) by Almond and coworkers [53], 55 GPa by Yoshimoto and coworkers [77], 26.9 GPa (at 220 K) by Kim and coworkers [78], 56.3 GPa by Salomons and coworkers [79], and 50.2 GPa by Bridge and Round [88]. Using a bending method Alford and coworkers [85] measured the static Young modulus and estimated for fully dense YBCO that $E = 180$ GPa. The static Young modulus of polycrystalline YBCO was also measured by Chang and coworkers [90] using Hertzian loading. They found at room temperature $E = 226$ GPa. Other reported elastic constants of polycrystal YBCO are listed in Appendix A. Some argue that material defects explain the different results among the methods applied. The material defects include voids, twins, microcracks, nonhomogeneities, texture, and residual stress. Recently, Ledbetter and Lei [174] discussed this problem and concluded that the ultrasonic-velocity bulk modulus is more realistic because it is consistent with many physical properties: atomic volume, cohesive energy, thermal expansivity, Debye temperature, and Grüneisen parameter. For the YBCO bulk modulus, they estimated that $B = 107$ GPa.

The studies on temperature dependence of sound velocity and elastic moduli show different results. Ledbetter and coworkers [54] measured the shear modulus of polycrystalline YBCO between 275 and 4 K using a pulse-echo method. They found that above T_c the shear modulus shows normal behavior: it stiffens with decreasing slope during cooling, consistent with the Varshni relationship [175]. Similar results have been reported by other authors [56–61,63,65–67,70,71,74,77,78,94,95,98–100,107–109,113,121,122, 126,131,132,140]. Such a dependence of the elastic moduli has been observed in single crystals [93,110,114,115].

During cooling below T_c, however, Ledbetter and coworkers [54] found an abnormal behavior of the shear modulus: the slope increases after it approaches zero. This behavior can be described by a "reentrant softening" model [176]. The increased stiffness below the critical transition temperature is the result of the softening being offset by the increased stiffness associated with the developing superconducting phase. The calculated Debye temperature based on this model agrees with other experimental measurements. Also, this model predicts that elastic constants in the superconducting state will be lower than those in the normal state, consistent with the thermodynamics of second-order phase transitions.

Strong thermal hysteresis in acoustic frequency and sound velocity was observed by many researchers [53,59,73,92,95,106,117,135,147,149,177,178]. The cause of the hysteresis remains unclear. Some authors [53,73,92,117,147] conjectured that this thermal hysteresis is caused by a phase transition or by the coexistence of tetragonal and orthorhombic phases [59].

The changes of elastic properties at transition temperature were found by some authors [63,76,97,143]. Remarkably, Migliori and coworkers [76] reported a large change of the resonant frequency at T_c, indicating a sharp drop in the sound velocity with increasing temperature at the phase transition. In contradiction, Lægreid and coworkers [50] did not observe any changes either in the sound velocity or in the slope of the sound velocity at T_c. Also, elastic softening in sound velocities above T_c were reported [75,95,102,177].

The reason for discord remains unclear. Possible reasons might be the following: (1) Different frequencies. The frequency range applied in an ultrasonic method varies from 1 kHz to 30 MHz. (2) Mixtures of different phases: orthorhombic I and orthorhombic II. These phases contain different oxygen content and they show different properties [179]. (3) Impurities, such as CuO. Anomalies of the temperature dependence of the sound velocity and elastic moduli may arise from a magnetic phase transition in CuO. (4) Hysteresis. Thermal history (and perhaps mechanical history) may affect YBCO's properties [92].

The anomalous stiffening below T_c observed in polycrystals was also reported in single crystals [93, 110, 111, 113, 114]. Hoen and coworkers [93] suggested that the anomalous stiffening below T_c observed in polycrystalline samples is not due to integranular effects, but is intrinsic to $Y_1Ba_2Cu_3O_7$. Thermal hysteresis was also observed in a single-crystal specimen [93].

As for the monocrystal elastic constants, only one set of complete C_{ij} derived from the phonon frequencies of inelastic neutron scattering for a mean-tetragonal structure was reported [172]. Using sound-velocity measurements, Saint-Paul and coworkers [111] estimated C_{33} and C_{44}. Also from sound velocities, Golding and coworkers [113] calculated the pseudo-tetragonal elastic constants C_{11} and C_{33}. Baumgart and coworkers [170, 171] determined C_{11}, C_{33}, and C_{44} by Brillouin spectroscopy.

For YBCO, some model calculations were reported. Using the interatomic force constants, estimated from electronegativity values and bond lengths, and the crystal structure information, Bridge and Round [180] calculated the bulk modulus for single-crystal YBCO. They obtained $B = 253$ GPa.

This is much higher than the measured bulk modulus for the single-crystal specimen [173], 115 GPa. Valkealahti and coworkers [181] studied structural properties of YBCO by static-lattice simulation methods and found good agreement between the model calculations and the experimental results. Also, by simple ionic potentials, they studied elastic constants. The elastic and acoustic properties of a polydomain phase at the intrinsic ferroelectric phase transition in the YBCO were studied by Vitebskii and coworkers [182]. Starting from the mean-field free energy, Millis and Rabe [183] derived expressions for the singularities in the behavior of the lattice parameters and sound velocities near T_c. Their theory predicts the existence of three types of singularities at T_c: (1) a discontinuity in the temperature derivatives of the lattice parameters; (2) a discontinuity in the elastic moduli and sound velocities; (3) a discontinuity in the temperature derivatives of the elastic moduli and sound velocities. For YBCO, they found inconsistencies between the theory and the experimental results.

2.3 Other High-T_c Oxide Superconductors

$La_{2-x}Sr_xCuO_4$ (LSCO) is a compound quite similar to LBCO and has a higher T_c of approximately 40 K. After the discoveries of LBCO (LSCO) and YBCO, another two families of oxide superconductors with T_c above 100 K were found: Bi–Sr–Ca–O (BSCCO) and Tl–Ba–Ca–Cu–O (TBCCO). Although the compositions and the properties of the four types of materials are different, they have common features—CuO_2 sheets of corner-linked square-planar-coordinated copper, and oxygen nonstoichiometry or cation disorder in layers that interleave the CuO_2 sheets.

Studies similar to those for YBCO have been done for the other three families: the temperature dependence of elastic moduli and sound velocities for LSCO [56,100,104,105,107,115,116,118,133,161,184–196], BSCCO [98, 115, 160, 197–202], and TBCCO [203]; temperature dependence of internal friction and attenuation for LSCO [56, 100, 104, 107, 133, 187–195], BSCCO [98, 160, 169, 197, 198, 200, 204], TBCCO [205]; and the room-temperature elastic constants and sound velocities for LSCO [78,80,161,190,206–208] and BSCCO [160,171,201,202].

Studies have shown different elastic constants for LSCO and BSCCO as for YBCO. For example, for LSCO, a megahertz pulse-echo method finds

the bulk modulus to be 137 GPa [161] at room temperature; but a vibrating-reed method yields 160 GPa [190]. Even the same method gives different results sometimes. By high-pressure study, Takahashi and coworkers [207] reported 135 GPa for the bulk modulus, while Dietrich and coworkers [80] found $B = 160$ GPa. For $(Bi\text{–}Pb)_2Sr_2Ca_2Cu_3O_{10+x}$, the bulk modulus was reported to be 17.4 [160] and 9.7 GPa [201] both by pulse-echo method.

The elastic moduli and sound velocities for LSCO show strong softening when temperature is decreased [161, 184, 185, 189–196], especially the shear modulus softens up to 30% [161]. This lattice softening is usually ascribed to a structural instability [184, 190].

For BSCCO, the measured sound velocities and elastic moduli show stiffening when temperature decreases in both polycrystals [98, 197, 201, 202] and monocrystals [115, 198–200].

Hysteretic behavior in sound velocities and elastic moduli was observed also in LSCO [189, 190], BSCCO [201, 202], and TBCCO [203].

2.4 Summary

Many studies have been done on elastic and related properties of $BaTiO_3$, $SrTiO_3$, and high-T_c metal-oxide superconductors, especially YBCO.

For the perovskites, the studies included room-temperature properties, temperature dependences, and model calculations. Despite all the efforts, no one measured the low-temperature elastic constants of $BaTiO_3$, to 4 K; and a phase transition near 40 K in $SrTiO_3$ remains controversial.

For the high-T_c oxide superconductors, the elastic properties display many complexities. For example, the reported bulk modulus of YBCO varies in a wide range: from 27 to 196 GPa. And the studies show different temperature dependences of elastic constants, especially the behavior near T_c. The reasons for discord need to be clarified.

Chapter 3

Materials and Measurement Methods

3.1 Materials

The specimens used for this study include monocrystal $SiTiO_3$, polycrystal $BaTiO_3$, and polycrystal YBCO superconductor.

The polycrystal $BaTiO_3$ and monocrystal $SrTiO_3$ specimens were obtained from commercial sources.

The YBCO specimen was prepared at Arkansas University by Z. Sheng. Well-mixed powders of Y_2O_3, $BaCO_3$, and CuO were heated at 925°C in air for 24 h. After being cooled slowly, the material was ground into fine powder and pressed to a tablet-shape. Then the tablet was put into a tube furnace with oxygen at 940°C for 12 h, and the temperature was kept at 650°C for another 2 h. Finally, the temperature was reduced to room temperature. Thickness of the tablet-shaped specimen is 2.6 mm. Figure 3.1 shows the electrical resistance and magnetic susceptibility for the specimen, which indicate that the superconducting transition occurs at 91 K. The oxygen content of the specimen was estimated from X-ray diffraction as 6.85, that is, the molecular formula for the specimen is $Y_1Ba_2Cu_3O_{6.85}$.

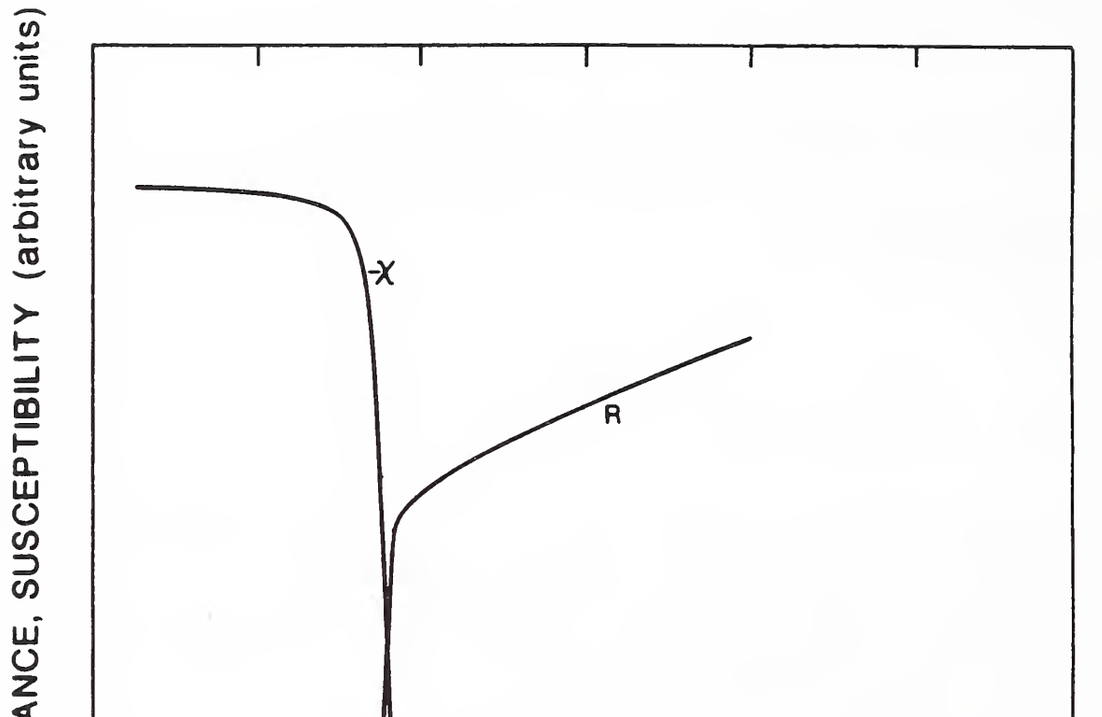

Figure 3.1: Temperature variation of electrical resistance and magnetic susceptibility of YBCO specimen.

3.2 Measurement Methods

3.2.1 Mass Density

The mass densities of $BaTiO_3$ and $SrTiO_3$ were determined by Archimedes's method using distilled water as a standard. Hence, density can be calculated from the following relationship:

$$\rho = \frac{M_o}{M_o - M_\ell}\rho_\ell. \tag{3.1}$$

Here, M_o and M_ℓ indicate specimen mass in the air and liquid, respectively; and ρ_ℓ denotes the density of liquid (distilled water), which can be found in handbooks. The inaccuracy of this method is estimated as 2 parts in 10,000. Due to the chemical reactivity with oxygen and water, instead of using Archimedes's method, the effective mass density of the YBCO superconductor was determined by measuring macroscopic dimensions and mass, with an inaccuracy of 4 parts in 10,000.

3.2.2 Acoustic-wave Velocity

To measure elastic constants, a megahertz-frequency pulse-echo method [209] was used. The ultrasonic wave velocity v is determined by

$$v = \frac{2l}{t}. \tag{3.2}$$

Here, l denotes specimen length and t denotes round-trip time for an ultrasonic pulse to travel between two flat-and-parallel specimen faces. The electric pulse is produced by a pulse generator and converted to an ultrasonic pulse by quartz and PZT piezoelectric transducers with frequencies between 3 and 10 MHz. The transducer is bonded to the specimen surface using phenyl salicylate and glycerine–alcohol. Figure 3.2 shows a diagram of the electronics system, and Fig. 3.3 shows a typical pulse-echo pattern. The travel time t is determined by measuring the time difference between consecutive echoes in a pulse-echo pattern using a dual-channel sweep-delayed time-interval-microprocessor-equipped oscilloscope with a 0.001 μs resolution.

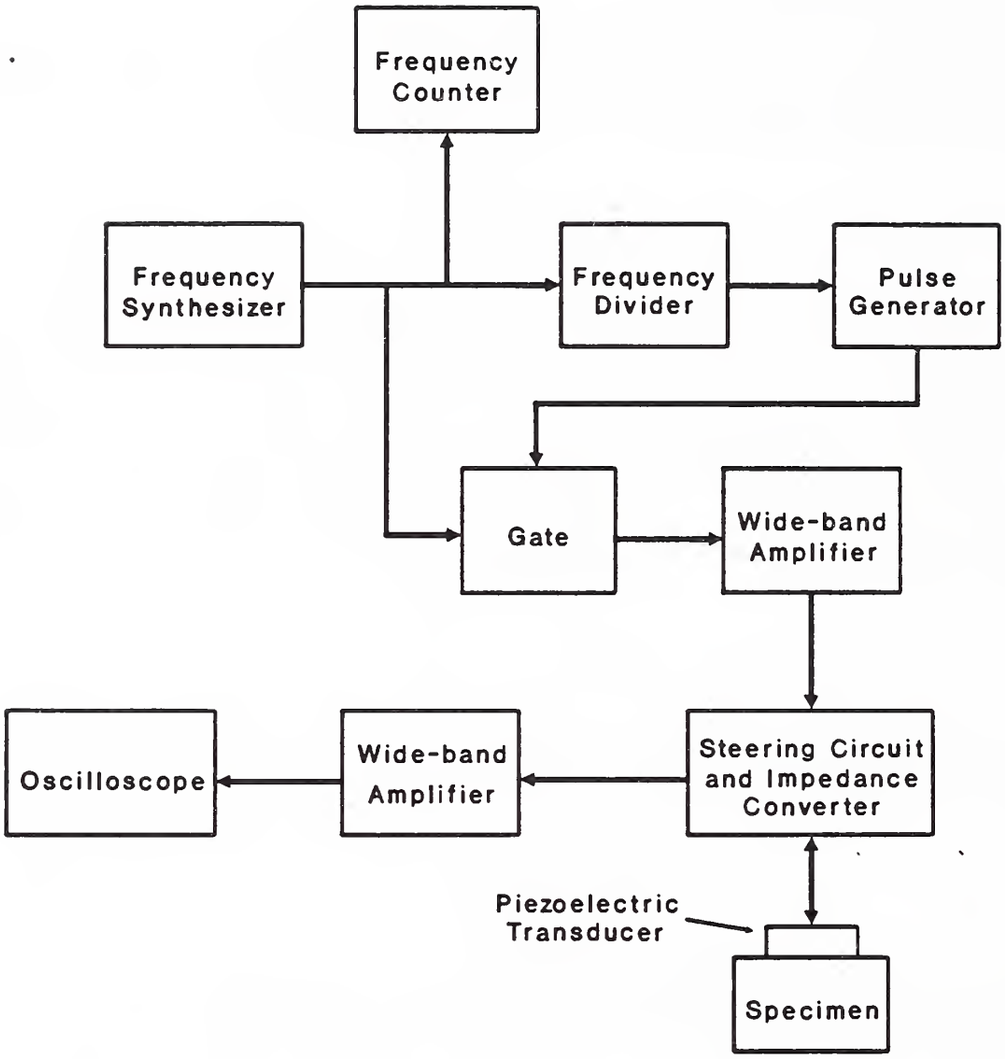

Figure 3.2: Functional diagram of ultrasonic pulse-echo sound-velocity-measurement system.

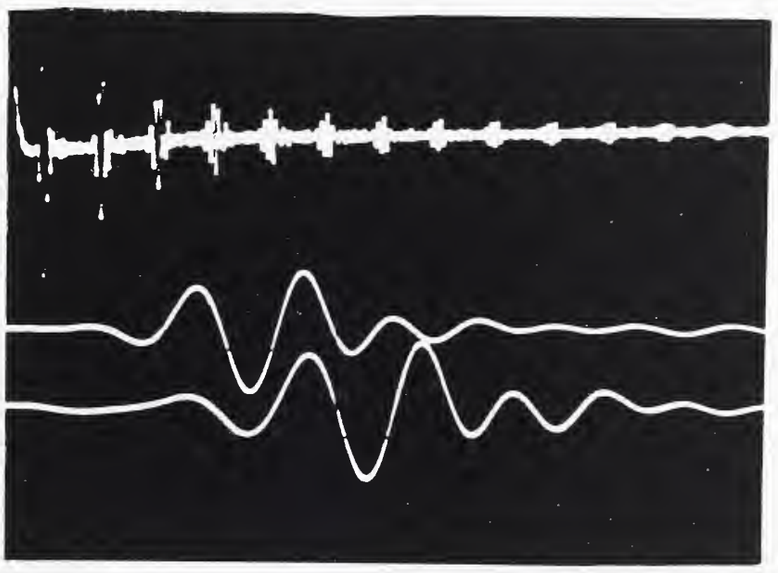

Figure 3.3: Composite oscilloscope display of transverse-wave pulse-echo pattern at 4 K for YBCO specimen. Expanded first and second echoes are shown at bottom. Transit time was measured between the first minimum in these adjacent echoes. Carrier frequency equals 4 MHz.

The elastic constants C can be calculated from the general relationship

$$C = \rho v^2. \tag{3.3}$$

For polycrystal $BaTiO_3$ and YBCO specimens, which possess isotropic symmetry, we need only two measurements: longitudinal velocity v_ℓ and shear velocity v_t. The longitudinal modulus C_ℓ and shear modulus G can be calculated from Eq. (3.3) by the substitution of v_ℓ and v_t, respectively. Then the bulk modulus B can be determined by

$$B = C_\ell - \frac{4}{3}G. \tag{3.4}$$

By using the interrelationships among isotropic-solid elastic constants, we can also obtain other engineering elastic constants: the Young modulus

$$E = \frac{9BG}{3B+G} = \frac{G(3C_\ell - 4G)}{C_\ell - G}, \tag{3.5}$$

and the Poisson ratio

$$\nu = \frac{E}{2G} - 1 = \frac{C_\ell - 2G}{2(C_\ell - G)}. \tag{3.6}$$

For a monocrystal $SrTiO_3$ specimen, which possesses cubic symmetry, there are three independent elastic constants, usually taken as C_{11}, C_{12}, and C_{44}. From the Voigt–Reuss–Hill [210] averaging method, the quasiisotropic elastic constants can be obtained from monocrystal results.

The inaccuracy of elastic-constant-measurement is estimated to be 5 parts in 10,000. This is based on measurements on standard monocrystal specimens such as aluminum and copper.

3.2.3 Low-temperature Measurements

To obtain the temperature dependence of elastic constants, a low-temperature probe was used. The probe was placed in the ullage of a helium dewar and lowered stepwise to achieve cooling. Temperatures were monitored with a chromel-constantan thermocouple contacting the specimen. Figure 3.4 shows the probe. The cooling rate was about 2 K/min.

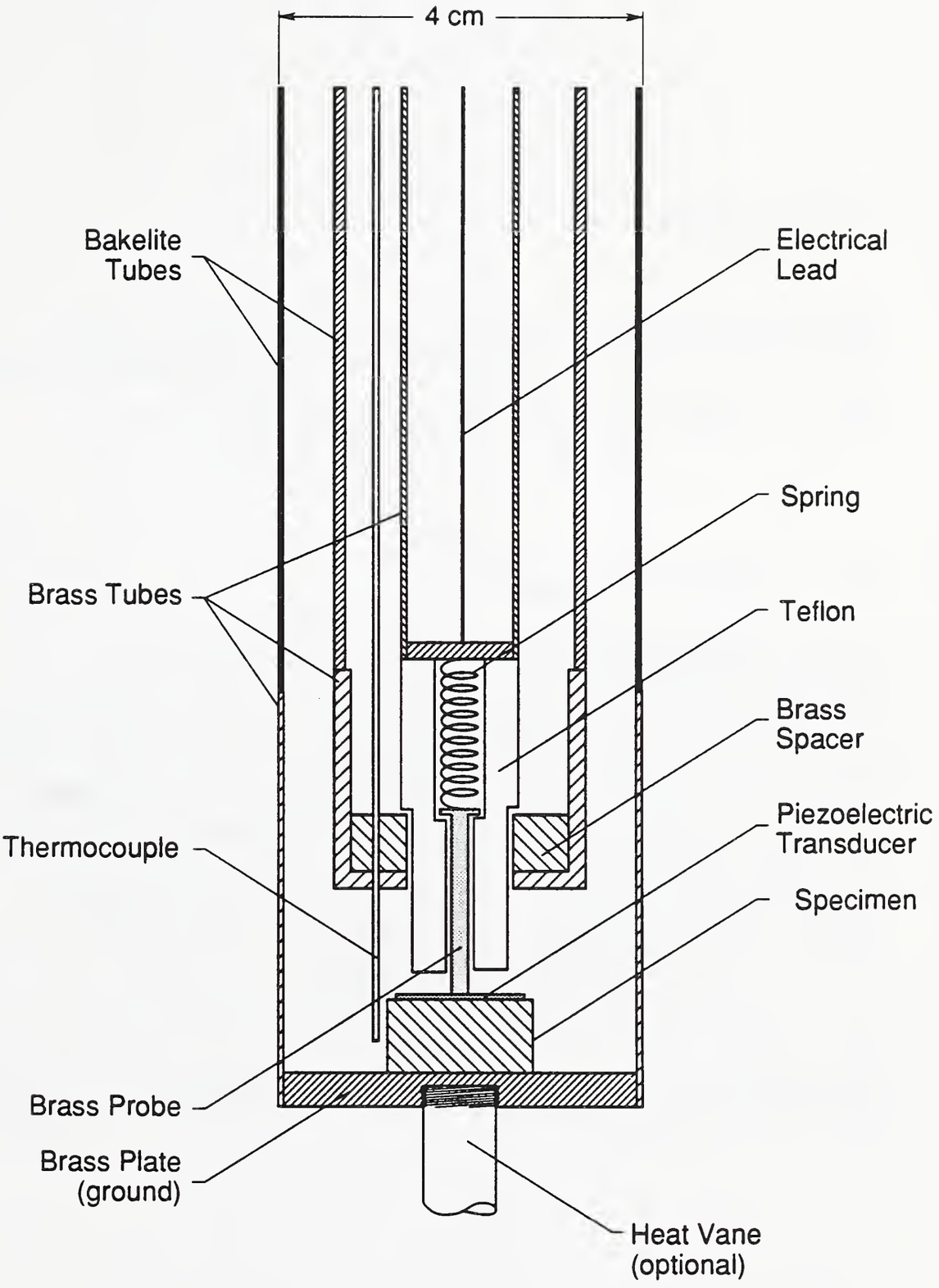

Figure 3.4: Low-temperature probe.

Chapter 4

Elastic-constant Measurement Results and Analysis

4.1 Perovskites

4.1.1 Polycrystal $BaTiO_3$

The temperature dependences of elastic constants of the polycrystal $BaTiO_3$ specimen in the range of 295–4 K are shown in Fig. 4.1. The elastic constants change smoothly within the temperature range without showing any anomaly. The elastic moduli of $BaTiO_3$ show large changes and stiffen with decreasing temperature, especially the shear modulus, which increases 28%. The Poisson ratio changes in a different way—decreasing about 14%.

The room-temperature elastic constants of the polycrystal are lower than those of a monocrystal reported by Huibregtse and coworkers [10]. Due to the thinness of the monocrystal specimen for the present study, only one elastic constant C_{11} was obtained, which is close to the results of Huibregtse and coworkers. Therefore, the monocrystal measurement results at room-temperature by Huibregtse and coworkers are preferred and tabulated in Table 4.1 for further use.

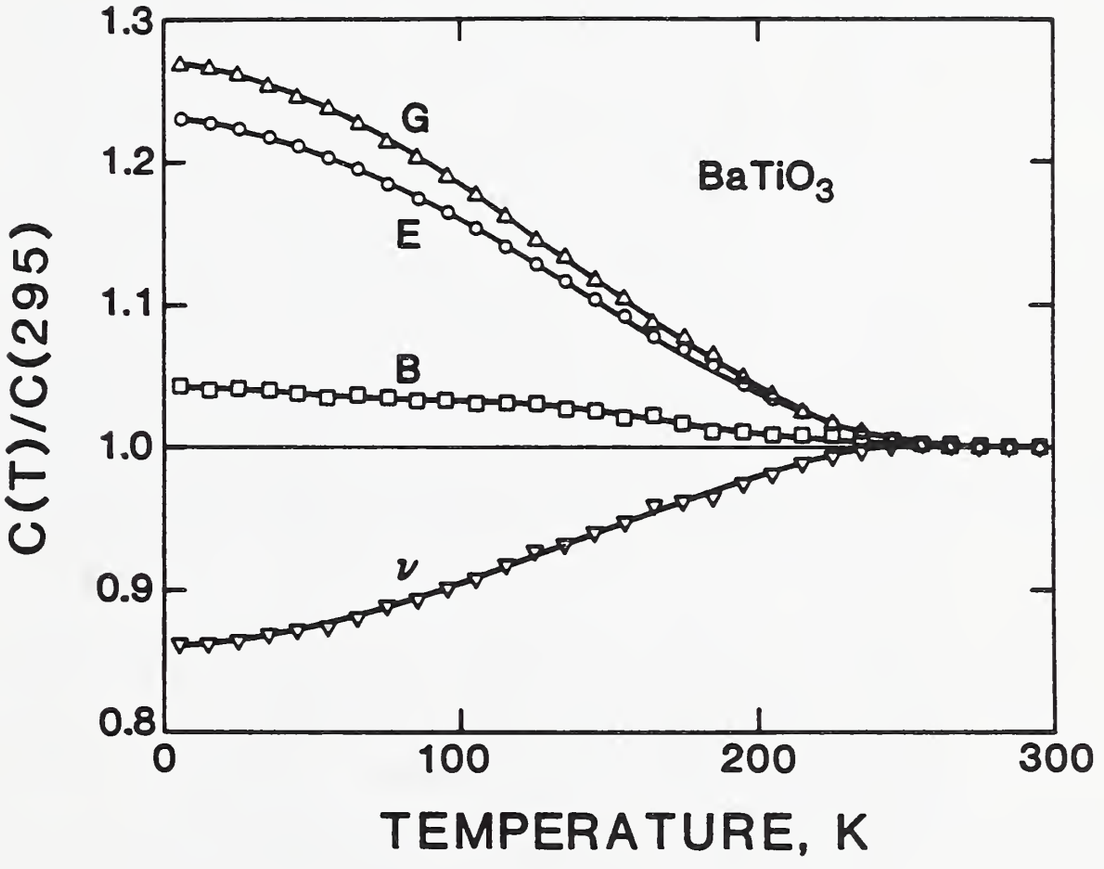

Figure 4.1: Temperature variation of elastic constants of polycrystal barium titanate.

Table 4.1: Measured elastic constants at T= 295 K.

	ρ	v_ℓ	v_t	C_ℓ	G	B	E	ν	$\bar{c}$
	(g/cm^3)	(cm/μs)	(cm/μs)	(GPa)	(GPa)	(GPa)	(GPa)		
$BaTiO_3$	5.998	0.596	0.356	213.06	75.24	166.67	196.20	0.304	–
$SrTiO_3$	5.110	0.812	0.480	336.70	117.60	179.90	289.68	0.232	–
YBCO	5.517	0.496	0.287	135.84	45.58	75.06	113.72	0.248	0.131
YBCO[a]	6.348	0.532	0.305	179.55	58.99	100.89	148.11	0.255	–

[a]Corrected to void-free state.

4.1.2 Monocrystal $SrTiO_3$

The measured elastic stiffnesses C_{ij} of monocrystal $SrTiO_3$ at ambient temperature agree well with those determined using the same method by Bell and Rupprecht [25] and by Wachtman and coworkers [26]. The quasiisotropic elastic constants calculated from the C_{ij} using the Voigt–Reuss–Hill [210] averaging method are listed in Table 4.1.

For the monocrystal $SrTiO_3$, Fig. 4.2 shows the temperature dependences of the elastic moduli and the Poisson ratio. In the temperature range 295–108 K, the elastic constants show similar behavior with that of $BaTiO_3$—E, G, B increasing and ν decreasing, in a smaller magnitude than $BaTiO_3$, with decreasing temperature. A cubic–tetragonal structure phase transition occurs at 108 K where the elastic moduli drop drastically. Below 108 K, the Young and shear moduli decrease further and reach a minimum at 66 K. Different from the behavior of Young and shear moduli, the bulk modulus increases below 108 K and reaches its first maximum at 66 K and the second maximum at 20 K. Unlike $BaTiO_3$, the Poisson ratio of $SrTiO_3$ shows a large increase below 108 K and goes through two maxima at 66 and 20 K, respectively. All the changes of elastic constants below 108 K indicate some kind of phase transitions occur in this region. Since little or no hysteresis was observed in $SrTiO_3$ specimen, these transitions may be approximately second order.

4.2 Polycrystal YBCO Superconductor

4.2.1 Ambient-temperature Measurements

The sound velocities and elastic constants of YBCO measured at room temperature are also tabulated in Table 4.1.

Since the polycrystalline oxide superconductor contains voids, the measured elastic constants must be corrected to the void-free state to get the intrinsic-material elastic constants. First, the porous ceramic superconductor was considered as a composite containing spherical particles—voids. Because the void density $\rho_p = 0$, the void volume fraction $\bar{c}$ can be determined from the X-ray mass density ρ_m and macroscopic density ρ:

$$\rho = \rho_m(1 - \bar{c}) + \rho_p\bar{c} = \rho_m(1 - \bar{c}). \tag{4.1}$$

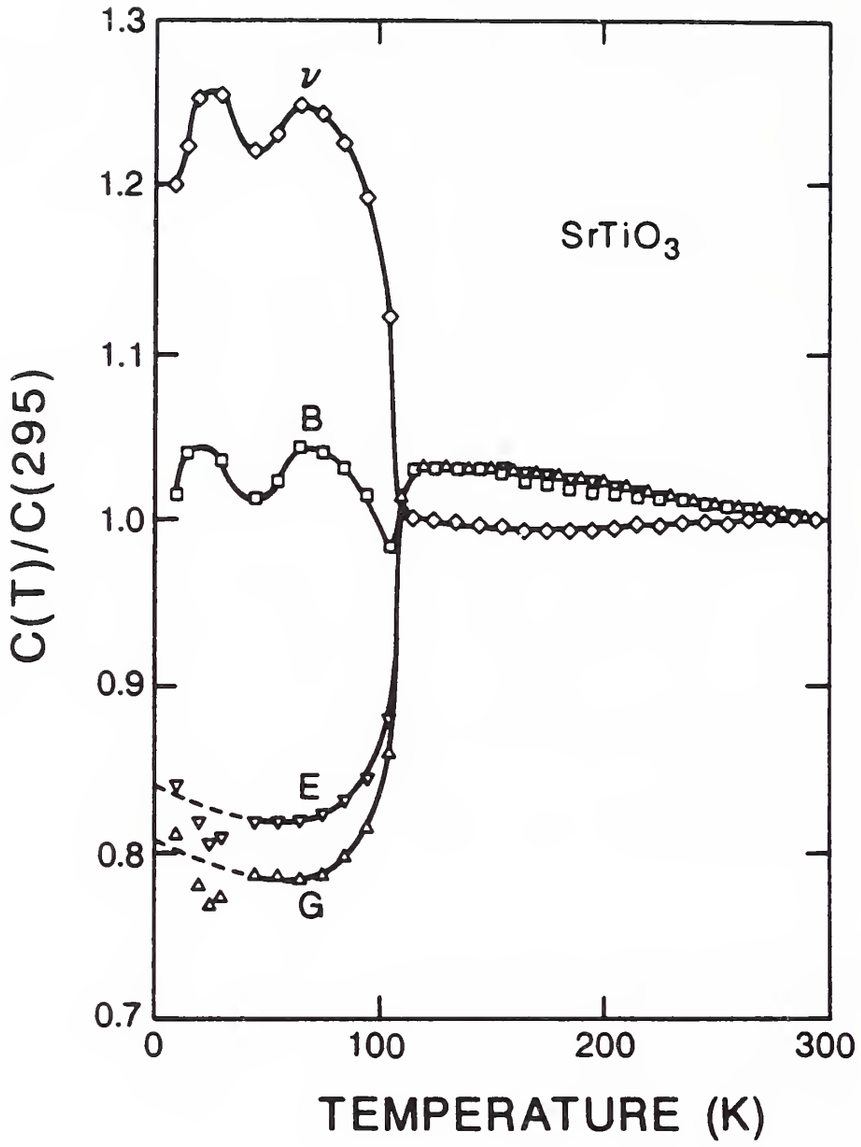

Figure 4.2: Temperature variation of elastic constants of monocrystal strontium titanate.

Here, the subscripts m and p denote matrix and particle.

Then, a model given by Ledbetter and Datta [211] for particle-reinforced composites was used to correct the measurements to the void-free state. Assuming randomly distributed spherical voids and taking the voids to possess zero elastic resistance to both dilatation and shear, we obtain expressions for shear and bulk moduli for a material containing spherical pores:

$$B = B_m \frac{4(1-\bar{c})G_m}{4G_m + 3\bar{c}B_m}, \tag{4.2}$$

and

$$G = G_m \frac{(1-\bar{c})(9B_m + 8G_m)}{(9+6\bar{c})B_m + (8+12\bar{c})G_m}. \tag{4.3}$$

Solving Eqs. (4.2) and (4.3) for G_m and B_m, we obtain the following results:

$$\frac{8}{3}(1-\bar{c})G_m^2 + \left[(3-2\bar{c})B - (\frac{8}{3}+4\bar{c})G\right] G_m - 3(1+\bar{c})BG = 0, \tag{4.4}$$

and

$$B_m = \frac{4G_m B}{4(1-\bar{c})G_m - 3\bar{c}B}. \tag{4.5}$$

Applying the usual quadratic-equation formula, Eq. (4.4) becomes

$$G_m = \frac{1}{2A_1}\left[-A_2 + (A_2^2 - 4A_1A_3)^{\frac{1}{2}}\right], \tag{4.6}$$

where

$$\begin{aligned} A_1 &= \frac{8}{3}(1-\bar{c}), \\ A_2 &= (3-2\bar{c})B - (\frac{8}{3}+4\bar{c})G, \\ A_3 &= -3(1+\bar{c})BG. \end{aligned} \tag{4.7}$$

Equations (4.5) and (4.6) represent bulk and shear moduli in the void-free state. Using Eqs. (3.5) and (3.6), we obtain the void-free Young modulus and Poisson ratio.

The corrected results are listed in the fourth row of Table 4.1. The corrected bulk modulus agrees well with the monocrystal measurement, 114.8 GPa, based on high-pressure X-ray diffraction, by Aleksandrov and coworkers [173].

Table 4.2: The fitted parameters of the moduli in the Varshni function.

	C_0 (GPa)	s (GPa)	Θ_E (K)
Bulk modulus B	105.98	3.25	147.91
Young modulus E	157.94	4.68	115.41
Shear modulus G	63.09	1.88	111.16

4.2.2 Low-temperature Behavior

Figure 4.3 shows the 295–4-K temperature dependences of elastic moduli and Poisson ratio of polycrystalline YBCO superconductor. Obviously, the elastic constants of the YBCO show very different temperature dependences from that of $SrTiO_3$. They also show smaller changes than $BaTiO_3$, the shear modulus of the YBCO increasing only about 7%, although they show a similar tendency with temperature. Against expectation, the elastic constants of this YBCO specimen showed practically no hysteresis. Similar to some previous studies, within the measurement error, no significant changes in the elastic stiffnesses were observed near T_c. But the Poisson ratio behaves otherwise. Near T_c, rather than decreasing smoothly during cooling, the Poisson ratio shows an irregular change: near 100 K it begins to decrease irregularly. This reflects some internal change in YBCO, because, among all the elastic constants, Poisson ratio shows the strongest sensitivity to changes in interatomic bonding.

The behavior of all the elastic stiffnesses of the polycrystalline YBCO obeys the Varshni function [175]

$$C_T = C_0 - \frac{s}{\exp(\Theta_E/T) - 1}. \tag{4.8}$$

Here, C_T and C_0 denote an elastic constant as a function of T and at zero temperature, respectively; s is a constant related to zero-point energy; and Θ_E denotes the Einstein temperature. Table 4.2 shows the fitting results for these parameters.

The following analysis shows that the parameter s can be calculated from some fundamental physical properties such as the Einstein temperature and

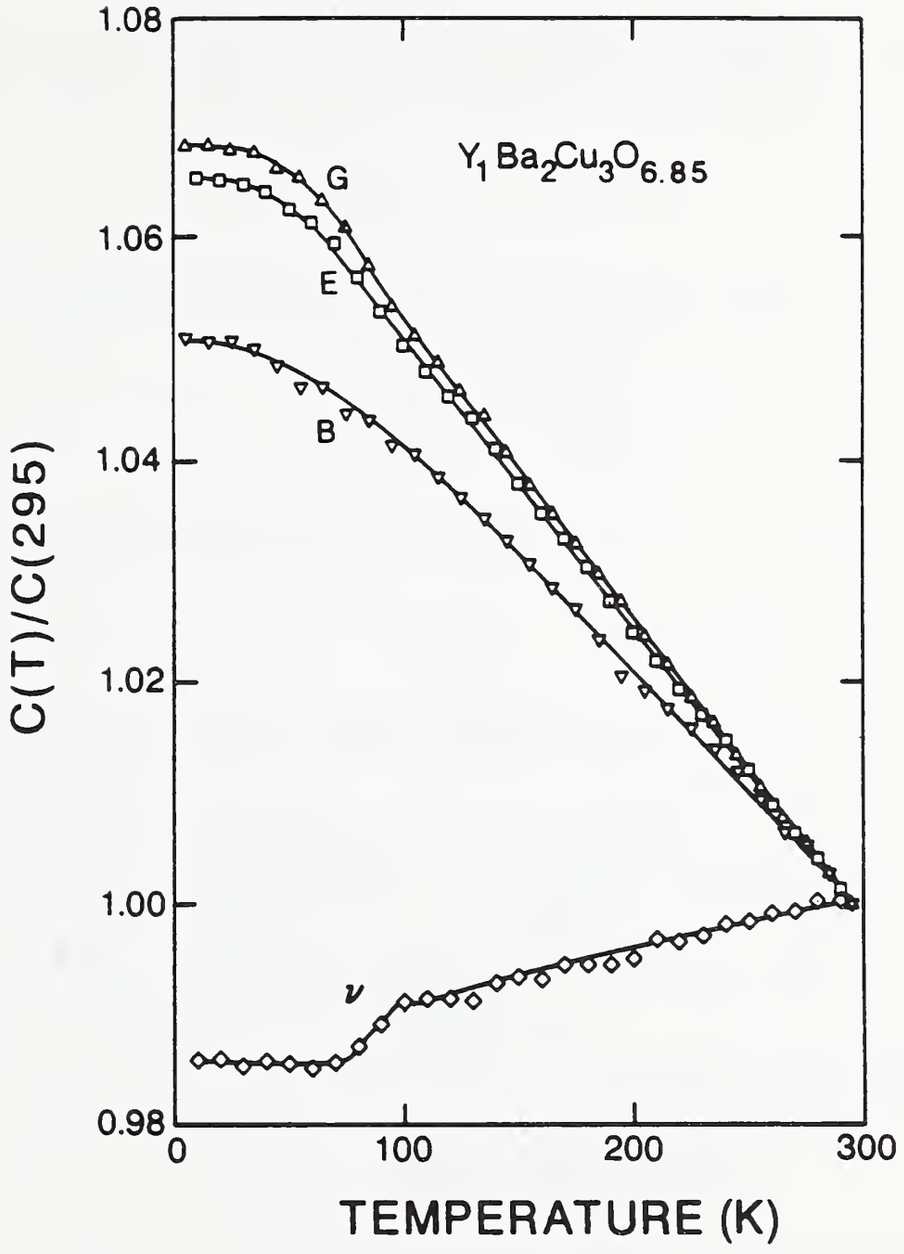

Figure 4.3: Temperature variation of elastic constants of polycrystal YBCO superconductor.

the Grüneisen parameter. The bulk modulus will be considered as an example. For the bulk modulus, in the high-temperature limit, Eq. (4.8) can be rearranged to the form

$$B_T = B_0 + \frac{s}{2} - \frac{s}{\Theta_E} T. \tag{4.9}$$

Figure 4.4 shows the the Varshni function and Eq. (4.9) for the bulk modulus. At zero temperature, Eq. (4.9) predicts that

$$\tilde{B}_0 = B_0 + \frac{s}{2}. \tag{4.10}$$

Here, $\tilde{B}_0$ denotes the harmonic-model value of the bulk modulus.

On the other hand, zero-point energy U_{zp} can be written as [212]

$$U_{zp} = \frac{9}{8} k \Theta_D. \tag{4.11}$$

Here, k indicates the Boltzmann constant. Then, we find the bulk modulus caused by zero-point energy:

$$B_{zp} = \tilde{B}_0 - B_0 = V_a \left(\frac{\partial^2 U_{zp}}{\partial V^2} \right)_{V=V_a} = \frac{9}{8} k \left(\frac{\partial^2 \Theta_D}{\partial V^2} \right)_{V=V_a}. \tag{4.12}$$

Since

$$\gamma \equiv -\frac{d \ln \Theta_D}{d \ln V}, \tag{4.13}$$

where γ is Grüneisen parameter,

$$\frac{d\Theta_D}{dV} = -\gamma \frac{\Theta_D}{V}. \tag{4.14}$$

Substituting Eq. (4.14) into Eq. (4.12), we obtain

$$\tilde{B}_0 - B_0 = \frac{9k\gamma(\gamma+1)\Theta_D}{8V_a}. \tag{4.15}$$

Comparing Eq. (4.15) with Eq. (4.10), yields an expression for s in terms of Einstein temperature, Grüneisen parameter, and atomic volume:

$$s = \frac{3k\gamma(\gamma+1)\Theta_E}{V_a}. \tag{4.16}$$

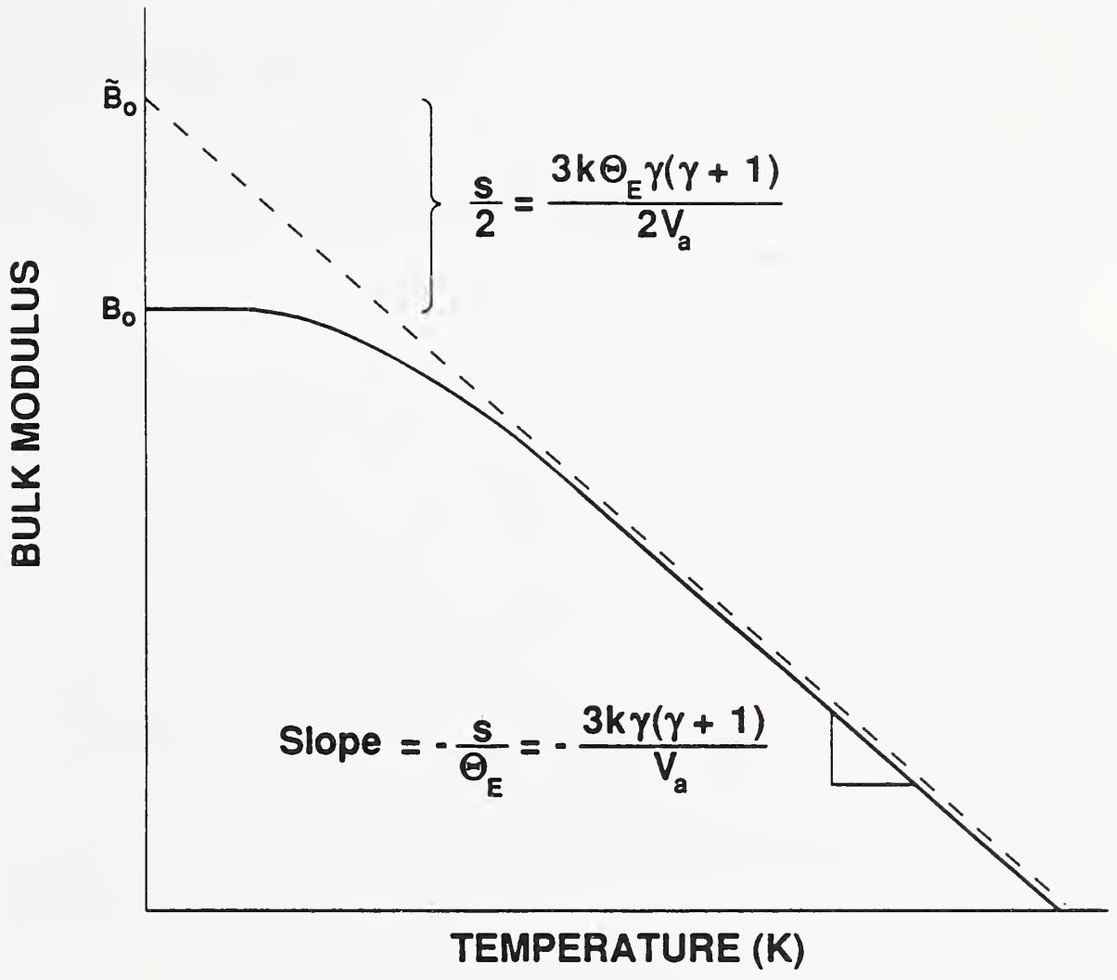

Figure 4.4: Schematic bulk-modulus–temperature curve in an Einstein-oscillator model. $\tilde{B}_0$ denotes the harmonic-model value of the bulk modulus.

In this equation, the relationship $\Theta_D = 4\Theta_E/3$ between Debye temperature and Einstein temperature was used.

For YBCO, the Debye temperature Θ_D is 440 K [213]. Hence, the Einstein temperature $\Theta_E = 0.75\Theta_D = 330$ K. Also for YBCO, Ledbetter [214] found that the Grüneisen parameter is around 1.35. Using these numbers for Θ_E and γ together with $V_a = 13.51$ Å^3 in Eq. (4.16), we find $s = 3.21$ GPa, which agrees well with the fitted value 3.25. The fitted Einstein temperature is lower than the value calculated from the measured Debye temperature. The reason for this is not known. Nevertheless, the Varshni function fits the measurements well. And the fitted result of s is in a good agreement with the simple Einstein-model calculation.

Chapter 5

Debye Temperature

The Debye characteristic temperature is a fundamental parameter that correlates with many physical properties of solids, such as specific heat, elastic constants, and melting temperature. Moreover, for superconductivity, as mentioned in the introduction, the Debye temperature relates to the electron–phonon parameter and to the critical transition temperature. Besides specific heat and elastic constants, there are various experimental methods to determine Debye temperature. For example, it can be determined using X-ray diffraction, Mössbauer effect, and electrical resistivity measurement. A complete review on this subject was given by Herbstein [215]. Here, only the elastic-constant method will be considered.

In Debye's theory, the Debye temperature Θ_D is defined through the cut-off frequency ν_D of the Debye spectrum for the elastic vibrations in an elastic continuum:

$$\Theta_D = \frac{h}{k}\nu_D. \tag{5.1}$$

Instead of considering a single frequency as proposed by Einstein, Debye assumed that the frequency distribution function takes the form

$$N(\nu)d\nu = \begin{cases} 4\pi\left(v_\ell^{-3} + 2v_t^{-3}\right)V\nu^2 d\nu & \nu \leq \nu_D \\ 0 & \nu > \nu_D \end{cases} \tag{5.2}$$

where $N(\nu)$ is the number of frequencies between ν and $\nu + d\nu$. With the constraint that the total number of normal vibrations must be $3N$, where N

is the number of atoms in the crystal,

$$\int_0^{\nu_D} N(\nu)d\nu = 3N. \tag{5.3}$$

Hence,

$$\nu_D = \left(\frac{3N}{4\pi V}\right)^{1/3} v_m, \tag{5.4}$$

where v_m is defined by Eq. (1.12). Substituting Eq. (5.4) into Eq. (5.1), we find Eq. (1.11).

For YBCO, using Eq. (1.11) and the mean sound velocity and the atomic volume given in Table 5.1, we find that $\Theta_D = 423$ K, which agrees well with the specific-heat Debye temperature, 440 K [213]. The Debye temperature at $T = 0$ K, Θ_D^0, can be obtained from the mean sound velocity at the same temperature by extrapolation of elastic constants using their temperature dependences. For YBCO, $\Theta_D^0 = 437$ K, which is almost identical with the specific-heat value. Theoretically, at $T = 0$ K, the Debye temperature calculated from elastic constants is exactly the same as that from specific heat [216]. Table 5.1 shows also the calculated Debye temperatures from elastic constants for $BaTiO_3$, $SrTiO_3$, LSCO, and BSCCO.

Figure 5.1 shows the temperature dependence of Θ_D calculated from measured elastic-constant temperature dependences. These three materials show strongly different behavior. For $BaTiO_3$, Θ_D increases smoothly about 12%. But, for $SrTiO_3$ Θ_D decreases about 10%, with a sharp decrease near 108 K caused by the paraelectric–improper-ferroelastic transition. As for YBCO, Θ_D increases almost linearly about 3% and shows no discontinuity around T_c.

Table 5.1: Sound velocities, bulk moduli, Debye temperatures, and electron–phonon parameters.

	T_c (K)	v_m (cm/μs)	B (GPa)	V_a (Å^3)	E_M (GJ/m^3)	Θ_D^{295} (K)	Θ_D^0 (K)	B_{calc} (GPa)	λ
$BaTiO_3$	–	0.394	166.7	12.91	−440.97	497	–	164	–
$SrTiO_3$	<1	0.532	179.9	11.91	−491.28	693	627	183	0.20
$BaPb_{0.75}Bi_{0.25}O_3$	12	–	–	15.77	−370.85	–	195[a]	138	0.70
$La_{1.85}Sr_{0.15}CuO_4$	38	0.346	137.4	13.43	−318.34	434	368	118	1.04
$Bi_2Sr_2Ca_1Cu_2O_8$	82	–	–	14.80	−251.27	–	240[a]	94	4.66
$Y_1Ba_2Cu_3O_{6.85}$	91	0.339	100.9	13.51	−262.93	423	437	98[b]	2.24
$(Bi–Pb)_2Sr_2Ca_2Cu_3O_{10}$	105	0.253	45.7	14.24	−257.78	312	319	96	4.39
$Tl_2Ba_2Ca_2Cu_3O_{10}$	125	–	–	15.64	−262.92	–	270[a]	98	7.82

[a]Elastic constants not measured. Specific-heat Θ_D from Fisher and coworkers [217].

[b]Calculated for $O_{7.0}$.

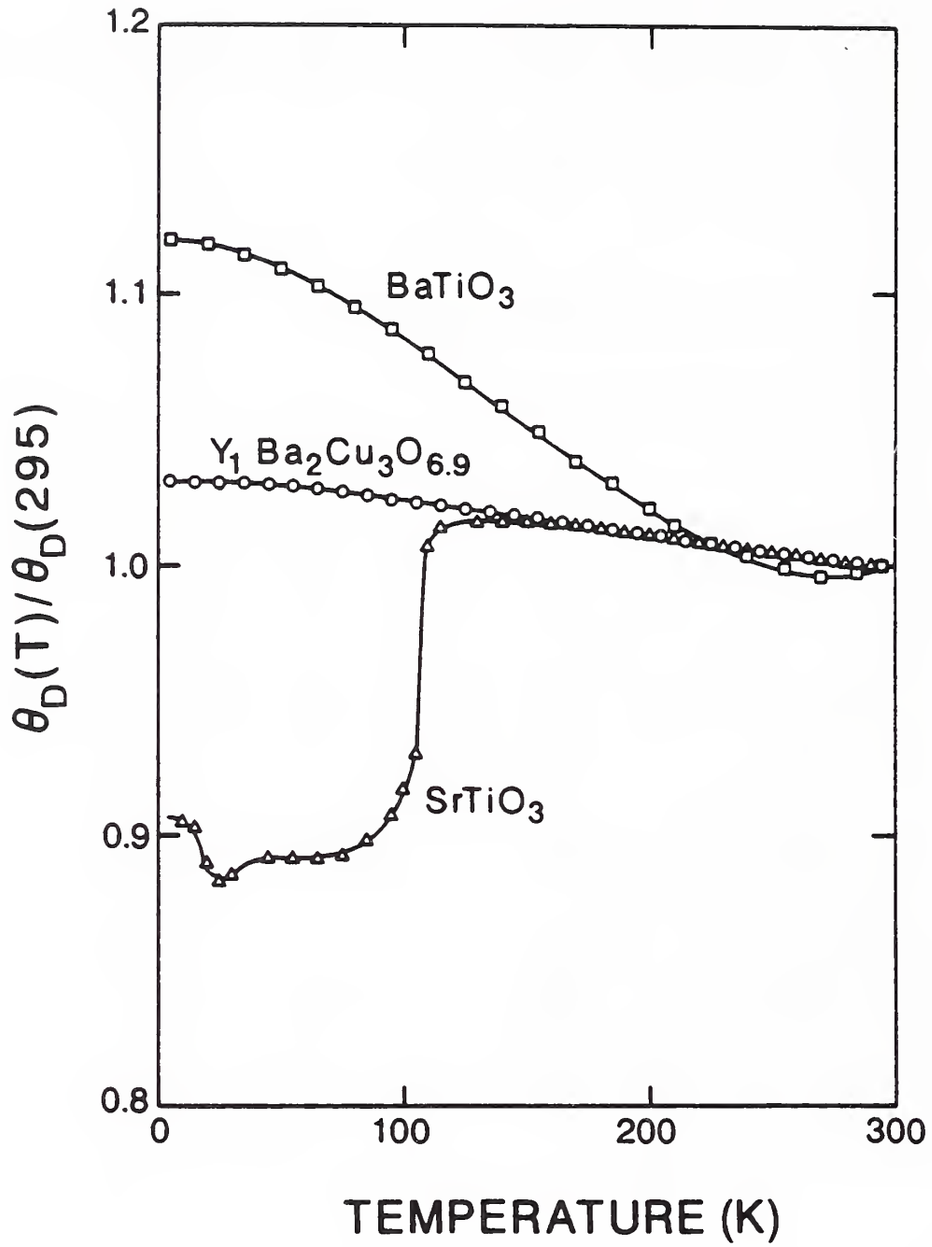

Figure 5.1: Temperature variation of Debye temperature for $BaTiO_3$, $SrTiO_3$, and YBCO superconductor. The absolute Θ_D values at room temperature appear in Table 5.1.

Chapter 6

Bulk Modulus

6.1 Calculation from Madelung Energy

6.1.1 Born Ionic Model

In general, there are two kinds of interactions between particles in a crystal: attraction and repulsion. The first is usually long range, while the second is usually short range. Atomic bonds due to these two interactions can be divided into primary and secondary in terms of interaction strength. Primary bonds include ionic, covalent, and metallic. Van der Waals and hydrogen bonds are considered secondary, being much weaker. For an ionic crystal, according to the Born model, the atomic interaction potential φ_{ij}, contains only two energy terms and can be written as (see Brown [218])

$$\varphi_{ij} = \pm\frac{Z_i Z_j e^2}{r_{ij}} + \frac{b'}{r_{ij}^n}. \tag{6.1}$$

Here, Z_i is the charge number of the ith ion; b' is a constant and n the Born exponent; e indicates electronic charge and r_{ij} denotes the distance between ions. Then, the lattice energy, U, can be determined by considering the contributions from each ion:

$$U = \frac{1}{2}\sum_i \sum_j{}' \varphi_{ij} = -\frac{Me^2}{r} + \frac{b}{r^n}. \tag{6.2}$$

Here, $\sum_j'$ indicates a sum not including $j = i$; r denotes the nearest-neighbor distance, b the repulsive constant, M the Madelung constant, which depends

only on the crystal structure. In Eq. (6.2), the first term represents long-range point-charge Coulomb interactions and is often called the Madelung energy. The second term is the short-range core–core repulsion interaction, often called the Born–Mayer repulsive energy. At equilibrium,

$$\left(\frac{dU}{dr}\right)_{r=r_0} = \left(\frac{Me^2}{r^2} - \frac{nb}{r^{n+1}}\right)_{r=r_0} = 0, \tag{6.3}$$

so

$$b = \frac{Me^2}{n} r_0^{n-1}. \tag{6.4}$$

Then, Eq. (6.2) becomes

$$U = -\frac{Me^2}{r}\left[1 - \frac{1}{n}\left(\frac{r_0}{r}\right)^{n-1}\right]. \tag{6.5}$$

Therefore, the bulk modulus is determined by

$$B = V_a\left(\frac{\partial^2 U}{\partial V^2}\right)_{V=V_a} = -\frac{E_M}{9V_a}(n-1). \tag{6.6}$$

Here, V_a denotes atomic volume, and

$$E_M = -\frac{Me^2}{r_0} \tag{6.7}$$

is the Madelung energy.

6.1.2 Madelung Energy

To calculate bulk modulus using Eq. (6.6), the Madelung energy (or the Madelung constant) has to be calculated. Because of long-range electrostatic interactions, the series of terms in the evaluation of the Madelung constant converges slowly. Several methods (direct and indirect) for evaluating the Madelung constant exist. In 1921, Ewald [219] introduced a general method that involves the reciprocal lattice and achieves rapid convergence. Although the Madelung constants for most simple crystal structures are known, they are unknown for general ionic charges and for complicated crystal structures. In this study, an Ewald method described by van Gool and Piken [220] was

used to calculate the Madelung constants for perovskitelike metal-oxide superconductors, especially YBCO.

To verify the computer program, the Madelung constants were calculated for all the crystal structures listed by Tosi [221], the perovskite crystal structures reported by Naimon [222], and the oxide-superconductor crystal structures considered by Iguchi and Yonezawa [223]. For all cases, the previous results were reproduced.

For this study, the unit-cell dimensions, ionic positions, and labeling for YBCO established by David and coworkers [224] were adopted. Figure 6.1 shows the crystal structure for orthorhombic $Y_1Ba_2Cu_3O_7$.

For valences, we chose that +3 for Y; +2 for Ba, Cu1, and Cu2; −2 for O1 and O4; and −1.75 for O2 and O3. These choices are discussed in Chapter IX.

6.1.3 Bulk Modulus

Before the bulk modulus can be calculated from Eq. (6.6), we also have to estimate the Born exponent for YBCO. For oxides, the Born exponent n was reported in the range between 3.79 and 4.95 [225]. For $BaTiO_3$ and $SrTiO_3$, from the the Madelung energies and the measured bulk moduli, n were estimated to be 4.40 and 4.30, respectively. Hence, the average, 4.35, was taken to be the Born exponent for YBCO. With the atomic volume V_a = 13.51 Å^3 and the Madelung energy $E_M = -283.98$ eV/molecule, we find the bulk modulus $B = 97.9$ GPa. This result agrees well with the measurements of both polycrystal, 100.9 GPa (see Table 4.1), and monocrystal, 114.8 GPa [173].

6.2 Comparisons with Other Oxides

As described in Chapter II, the reported bulk modulus for polycrystal YBCO varies in a wide range: from 27 to 196 GPa. The result given by the present study is much lower than those obtained from high-pressure studies. It is necessary to clarify what is the true bulk modulus of YBCO.

Since $BaTiO_3$ and $SrTiO_3$ are the crystal-structure building blocks for YBCO, it is useful to compare the bulk modulus for YBCO with those for the perovskites. Table 4.1 shows that the bulk modulus for YBCO is

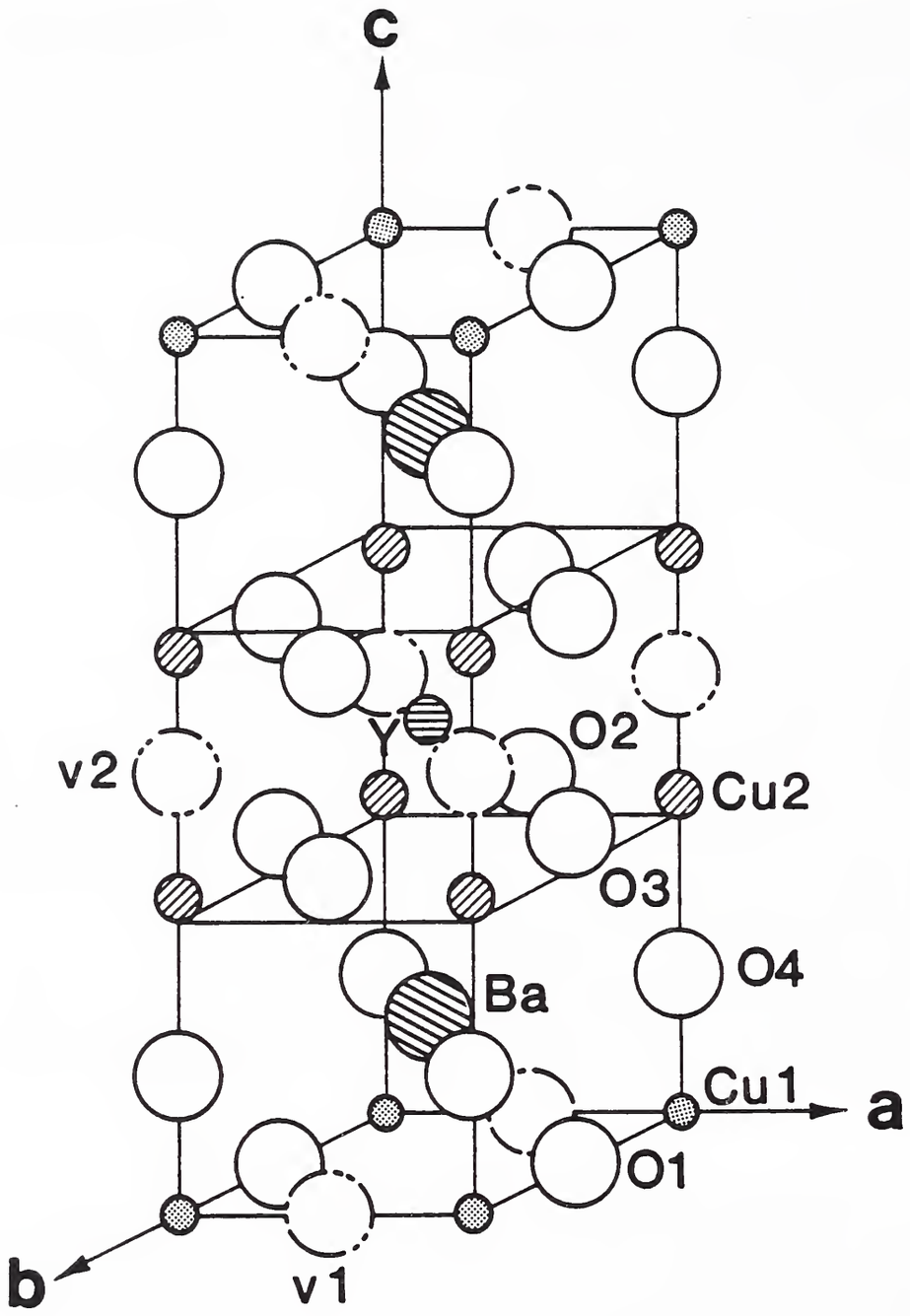

Figure 6.1: Crystal structure of $Y_1Ba_2Cu_3O_7$ showing one unit cell.

lower than those for $BaTiO_3$ and $SrTiO_3$. This is not surprising because the YBCO structure is formed approximately by stacking three unit cells of perovskite and removing two oxygen atoms. Such a structure essentially must be elastically softer than the complete structure, as typified by $BaTiO_3$ and $SrTiO_3$. Furthermore, for the real superconductor $Y_1Ba_2Cu_3O_{7-\delta}$, δ is between 0 and 0.5; thus, an additional oxygen site is occupied incompletely. In YBCO, although some Cu–O bonds are shorter, hence stronger, than in CuO, a structure's overall macroscopic stiffness depends more strongly on the weaker links: Y–O bonds, Ba–O bonds, and especially the missing Cu–O bonds.

Studying many monoxides and perovskites, Ledbetter and Lei [174] found a correlation between bulk modulus and cation–anion bond distance shown in Fig. 6.2. In YBCO, there are 27 metal–oxygen bonds (8 Y–O, 10 Ba–O, 9 Cu–O). Table 6.1 shows these bond distances given by David and coworkers [224].

Table 6.1: Bond distance and bulk modulus for YBCO.

Bond	Distance (Å)	N	B (GPa) ($= 3630/r^4$)
Y–O3	2.387	4	111.81
Y–O2	2.402	4	109.05
Ba–O4	2.741	4	64.31
Ba–O1	2.877	2	52.98
Ba–O3	2.949	2	48.00
Ba–O2	2.986	2	45.66
Cu1–O4	1.843	2	314.63
Cu1–O1	1.942	2	255.22
Cu2–O2	1.929	2	262.17
Cu2–O3	1.958	2	246.98
Cu2–O4	2.306	1	128.37

Using the bond lengths in Table 6.1 together with the curve in Fig. 6.2, we find that for YBCO the bulk modulus equals 138 GPa. However, this calculation was done with an assumption of a rocksalt-structure coordination number: six. Correcting the strong Cu–O bonds for reduced coordination

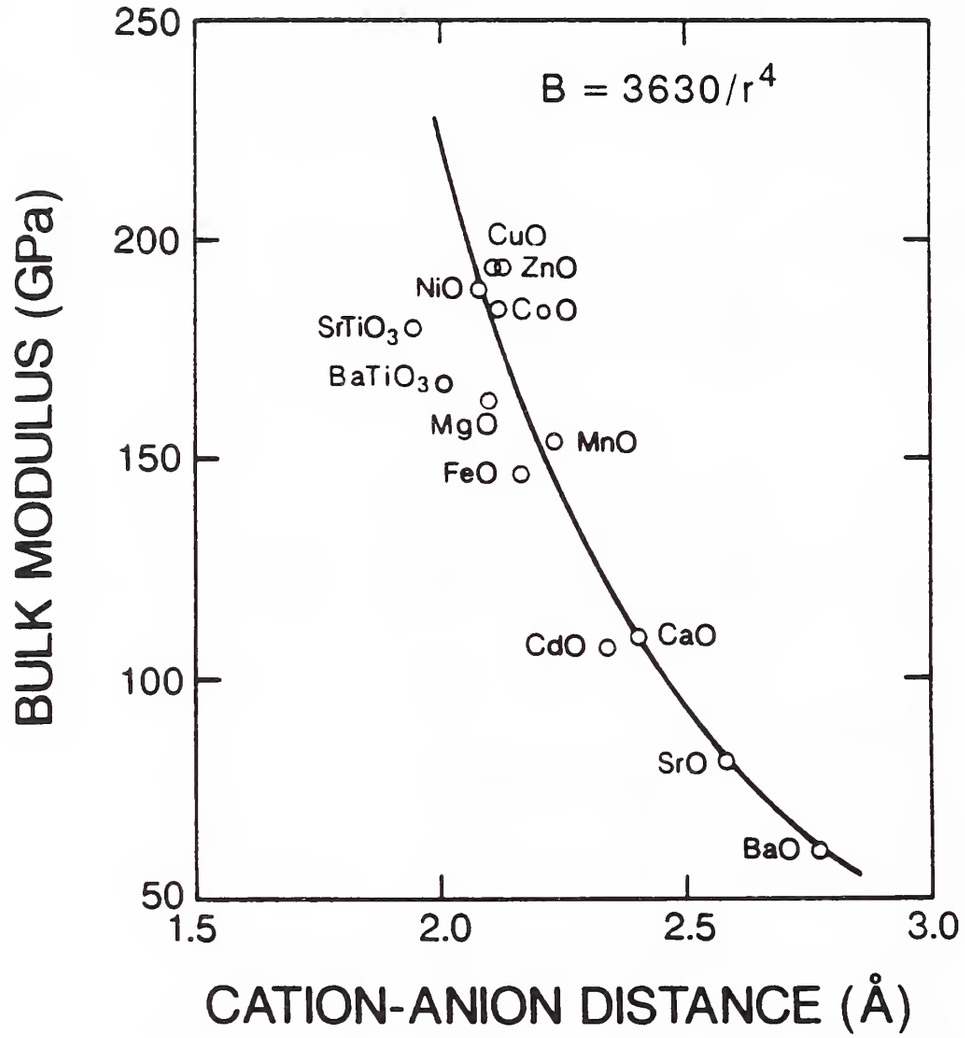

Figure 6.2: Dependence of bulk modulus on cation–anion distance for some oxides.

number (four and five) leads to $B = 116$ GPa, close to the measured bulk modulus $B = 101$ GPa.

Chapter 7

Monocrystal Elastic Constants of Orthorhombic YBCO

In the previous chapter, the bulk modulus of YBCO was discussed. Here, we consider the monocrystal elastic constants C_{ij}.

Since the YBCO superconductor possesses orthorhombic symmetry (space group $Pmmm$, no. 47), it exhibits nine independent C_{ij}. Although many studies have been done on both polycrystal and monocrystal YBCO, only one set of complete C_{ij} was reported, as mentioned in Chapter II. Table 7.1 shows the results reported by Reichardt and coworkers [172]. Although useful, the results reported by Reichardt and coworkers present some problems. First, their C_{ij} were obtained for a mean-tetragonal structure, thus only six out of nine independent C_{ij}. Second, the bulk modulus obtained from their C_{ij} by Voigt–Reuss–Hill [210] averaging disagrees with the monocrystalline-measurement, $B = 115$ GPa, reported by Aleksandrov and coworkers [173]. Third, errors in elastic constants determined from phonon-dispersion-curve slopes $d\omega/dk$ are usually larger than those measured ultrasonically.

Table 7.1 shows also some incomplete C_{ij} reported by other authors [111, 113,170,171].

Here, for orthorhombic YBCO, an estimate of C_{ij} based mainly on measurements on monocrystals combined with some analysis–theory was made. Polycrystal measurement results were excluded. Especially, all high-pressure measurement results were avoided since they present some problems [174], not yet understood, related perhaps to pressure-induced phase transitions.

Table 7.1: Measured and estimated monocrystal elastic constants for YBCO superconductor. Units are GPa for C_{ij} and TPa^{-1} for S_{ij}.

Source	C_{11}	C_{22}	C_{33}	C_{44}	C_{55}	C_{66}	C_{12}	C_{13}	C_{23}	B	β_1	β_2	β_3
Aleksandrov et al. [173]										115	2.43	2.10	4.21
Baumgart et al. [170, 171]	211		159	35									
Golding et al.[a] [113]	234		145										
Reichardt et al. [172]	230	230	150	50	50	85	100	100	100	131			
Saint-Paul et al. [111]			160	25									
Present	223	244	138	61	47	97	37	89	93	115	2.44	2.11	4.24

[a]Measured at 80 K.

The ultrasonically measured C_{11} and C_{33} by Golding and coworkers [113] (see Table 7.1) were adopted. Since these two elastic constants were measured at 80 K, they have to be adjusted to ambient temperature. Applying the polycrystal ratio $C_\ell(80)/C_\ell(295) = 1.05$, we find that at room temperature $C_{11} = 223.4$ GPa and $C_{33} = 138.4$ GPa, respectively.

From a ratio $C_{22}/C_{11} = 1.091$ calculated by Baetzold [226] from an empirical two-body-potential method, C_{22} was determined.

To determine C_{12}, C_{13}, and C_{23}, a simple elastic problem was considered. For a hydrostatic pressure P, Hooke's law gives

$$\begin{aligned} -P &= C_{11}\varepsilon_1 + C_{12}\varepsilon_2 + C_{13}\varepsilon_3, \\ -P &= C_{12}\varepsilon_1 + C_{22}\varepsilon_2 + C_{23}\varepsilon_3, \\ -P &= C_{13}\varepsilon_1 + C_{23}\varepsilon_2 + C_{33}\varepsilon_3. \end{aligned} \tag{7.1}$$

Solving these equations, we obtain

$$C_{12} = -\frac{a^2 C_{11} + (1-a)bC_{22} - C_{33} + (1-a-b)C_{23}}{a(1+b-a)}, \tag{7.2}$$

$$C_{13} = -\frac{a^2 C_{11} - b^2 C_{22} + (b-a)C_{33} - b(1+a-b)C_{23}}{a(1+b-a)}, \tag{7.3}$$

$$\begin{aligned} C_{23} = A\{&(a+ab-a^2)[9B_V - (C_{11}+C_{22}+C_{33})] \\ &+4a^2C_{11} - 2b(a+b-1)C_{22} - 2(1+a-b)C_{33}\}, \end{aligned} \tag{7.4}$$

where

$$A = \frac{1}{2[2(a+b+ab) - (1+a^2+b^2)]}. \tag{7.5}$$

Here, $a = \varepsilon_1/\varepsilon_3$ and $b = \varepsilon_2/\varepsilon_3$ are strain ratios. Using the three principal linear compressibilities

$$\beta_i = \sum_{j=1}^{3} S_{ij} \qquad i = 1,3 \tag{7.6}$$

found by Aleksandrov and coworkers [173] (see Table 7.1), we determined that $a = 0.58$ and $b = 0.50$. In Eq. (7.4),

$$B_V = \frac{1}{9}\left[C_{11} + C_{22} + C_{33} + 2\left(C_{12} + C_{13} + C_{23}\right)\right] \tag{7.7}$$

represents the Voigt-bound bulk modulus. We chose $B_V = 115.9$ GPa to make the Hill-average bulk modulus from the C_{ij}s equal the value of monocrystal measurement by Aleksandrov and coworkers.

To determine the three shear moduli C_{44}, C_{55}, and C_{66}, again, two C_{ij} ratios, $C_{44}/C_{66} = 0.633$ and $C_{55}/C_{66} = 0.485$, derived by Baetzold [226] were used. As above, more confidence was taken in Baetzold's C_{ij} ratios of diagonal terms than in his absolute C_{ij}s. The final problem then is to estimate C_{66}. The criterion was chosen that the Debye temperature calculated from the C_{ij} [5] equals the value determined from specific heat. Using the temperature dependence of the Debye temperature given in Chapter V and the value at 0 K (specific heat value) $\Theta_D^0 = 440$ K, we can obtain the value calculated from C_{ij} at room temperature $\Theta_D^{295} = 426$ K. Hence $C_{66} = 96.8$ GPa.

The estimated elastic constants for orthorhombic YBCO are shown in Table 7.1. Except C_{12}, the estimated C_{ij} differ from those measured by Reichardt and coworkers less than 10% on average. The large discrepancy between the estimated and measured C_{12} is unclear. Because C_{12} is not a simple elastic constant (no wave speed in the crystal depends only on C_{12}), it is difficult to calculate from basic principles and difficult to reason about on physical grounds.

Chapter 8

Electron–phonon Parameters

Electron–phonon interactions in solids play an important role in the theory of superconductivity. The interaction between electron and phonon is described by a parameter λ, called the electron–phonon coupling parameter. In conventional superconductors, electrons indirectly attract each other through exchanging phonons and form Cooper pairs, which are principally responsible for superconductivity. Therefore, the superconducting transition temperature T_c is sensitive to the electron–phonon interactions and the phonon frequency. Since the phonon describes the vibrations of the lattice, the phonon frequency strongly depends on the ion mass, M. Hence T_c is a function of ion mass. In fact, the isotope effect provides a simple relationship between T_c and ion mass: $T_c \sim M^{-\alpha}$, where α is a parameter. The isotope effect indicates that T_c approaches zero when $M \rightarrow \infty$. When the ion mass approaches infinity, ions can not move, hence, no lattice vibrations occur. Therefore, an isotope effect shows clearly that an electron–phonon interaction is the origin of superconductivity.

By measuring the isotope effect, Zettl and coworkers [115] studied the electron–phonon interactions in LSCO and YBCO high-temperature oxide superconductors. Within the error limits, they found shifts in T_c when replacing ^{16}O with ^{18}O and that $\alpha = 0.140 \pm 0.008$ and 0.023 ± 0.005 for LSCO and YBCO, respectively. The measured values of α for LSCO and YBCO are smaller than 0.5, a value expected from the conventional phonon–mediated paring mechanism. As described by Pickett [227], the isotope effect is not as simple as is usually assumed because "it involves not only the change in phonon frequencies but also the readjustment of the amount of retardation

of the electron–phonon interaction arising from the change in frequencies". In fact, several elemental superconductors show values of α strongly different from 0.5. For example, Zr and Ru have small values of α, near zero. α–U even shows a negative value. Therefore the small values of α for LSCO and YBCO can not exclude electron–phonon intreaction as a possible paring mechanism for oxide superconductors.

If it is assumed that electron–phonon interaction is responsible for superconductivity in high-T_c oxide superconductors, then λ can be estimated from T_c and Θ_D using the BCS relationship. However, the BCS expression was obtained for a weak-coupling approximation: $\lambda \ll 1$. The well-known McMillan [228] expression is valid up to $\lambda \cong 1$. The Allen–Dynes [229] expression applys only for $\lambda \geq 10$. Therefore, instead of either the BCS relationship or the McMillan or the Allen–Dynes relationships, the expression by Kresin [230] is preferred.

Directly from the Eliashberg equation, Kresin derived a simple analytical expression describing T_c for a full range of λ:

$$T_c = 0.25\Theta_D[\exp(2/\lambda) - 1]^{-1/2}. \tag{8.1}$$

Unlike the BCS, McMillan, and Allen–Dynes relationships, Kresin's relationship predicts that elastic softening always increases T_c.

Using the information of T_c and Θ_D in Table 5.1, the electron–phonon interaction parameter λ can be estimated from Eq. (8.1). The results are shown in Table 5.1.

Table 5.1 shows that the calculated lambdas vary over a wide range, from 0.20 for $SrTiO_3$ to 7.82 for TBCCO. The estimated values for λ in Table 5.1 provide a test as to whether an electron–phonon coupling mechanism can explain superconductivity in these oxides. If the lambdas are unreasonably large, then electron–phonon coupling is unlikely.

For LSCO, Rammer [231] calculated $\lambda \approx 2$ using a strong-coupling theory. From specific-heat measurements, Schlesinger and coworkers [232] estimated $\lambda \approx 1$–2. Using a method based on an analysis of heat capacity data, Kresin and Wolf [233] estimated that $\lambda \approx 1.8$–2.0. Using the Allen–Dynes relation, Horie and coworkers [58] found that $\lambda = 2.4$.

For YBCO, Rammer [231] similarly obtained $\lambda \approx 5$. Horie and coworkers [58] got an even higher value, $\lambda = 6.5$. Zeyher and Zwicknagl [234] calculated the superconductivity-induced phonon self-energy in the strong-coupling limit and found that $\lambda = 2.9$.

For BSCCO and TBCCO, no reported estimates of λ are available.

Independent calculations and estimates support the derived values of *lambda* from Kresin's expression, at least up to $\lambda \approx 5$. This leaves the highest value, $\lambda = 7.82$ for TBCCO, without theoretical or experimental support.

Figure 8.1 shows how T_c changes with λ. Besides the Kresin relationship, it shows lines representing the BCS, McMillan, and Allen–Dynes equations. As shown in the figure, almost for the full range of λ, from 2 to 10, BCS theory predicts too high a T_c, and McMillan too low a T_c. It is not a surprise because the values of λ in this range are beyond the limits of validity for both the BCS and the McMillan expressions. Figure 8.1 also shows that the Allen–Dynes curve lies near and parallel to the Kresin line. In fact, for large λ (strong-coupling limit), the Kresin relationship reduces to the form:

$$T_c = 0.177\Theta_D\lambda^{1/2}, \tag{8.2}$$

which is very close to the Allen–Dynes expression:

$$T_c = 0.182\Theta_D\lambda^{1/2}. \tag{8.3}$$

The behavior of the Kresin curve for strong coupling supports the Allen–Dynes contention that for large λ, $\lambda^{1/2}\Theta_D$, rather than λ, governs high T_c.

In the weak-coupling limit, the Kresin relationship fails to come to the BCS expression. Instead, it takes the form

$$T_c = 0.25\Theta_D \exp(-1/\lambda). \tag{8.4}$$

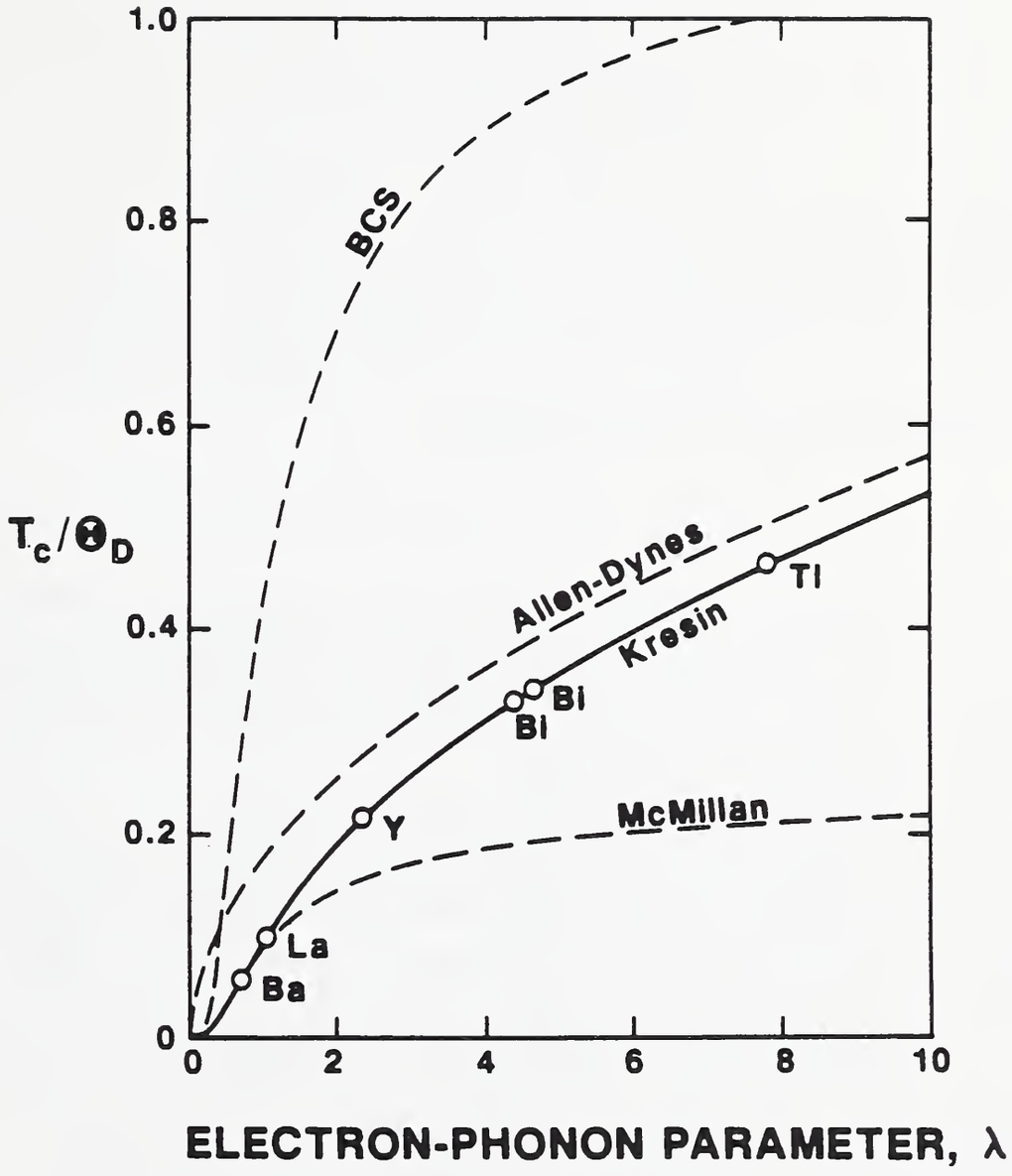

Figure 8.1: Variation of T_c/Θ_D with electron–phonon coupling parameter, λ. Points for seven oxide superconductors based on Kresin model. For comparison, the figure shows also curves from BCS (weak-coupling), McMillan (moderate-coupling), and Allen–Dynes (strong-coupling) models.

Chapter 9

Valence Problem

Superconducting properties in YBCO are very sensitive to the defect structure of oxygen ions, which determines the copper—oxygen ionic-charge configurations and the content of electron-hole carriers. Therefore, for understanding the mechanism of superconductivity in YBCO, it is important to know the ionic-charge distributions.

Calculations of lattice properties for high-T_c metal-oxide superconductors based on an ionic model were reported. By calculating the Madelung site potentials, Iguchi and Yonezawa [223] determined the most stable Cu^{+3} position and showed the remarkable stabilization of oxygen ions in $Y_1Ba_2Cu_3O_7$, compared with $Y_1Ba_2Cu_3O_8$. Wright and coworkers [235] focused on forces in $Y_1Ba_2Cu_3O_7$ and found that mechanical stability imposes constraints on copper-charge distribution. Kress and coworkers [236] predicted phonon-dispersion and phonon-density-of-states curves and concluded that interatomic interactions in $Y_1Ba_2Cu_3O_7$ resemble those in perovskites and other oxides. Further, they concluded that the ionic polarizability suggests strong electron—phonon interactions. Cohen and coworkers [237] considered lattice dynamics in La_2CuO_4 and $Y_1Ba_2Cu_3O_7$ and reached similar conclusions: important ionic contributions and large electron—phonon matrix-element enhancements. Also, they failed to find evidence for Cu^{+3}. Using a Madelung site-potential calculation, Kondo and coworkers [238] considered the hole-carrier distribution and found that the holes enter the CuO_2 plane.

For present purposes, the Madelung site potentials were calculated to determine the possible valence configuration for $Y_1Ba_2Cu_3O_7$. The Madelung

site potential for the ith ion is defined by

$$\Phi_i = \sum_{j \neq i} \frac{Z_i Z_j e^2}{| \vec{r_j} - \vec{r_i} |}. \tag{9.1}$$

The same computer program mentioned in Chapter VI was used for the calculation.

Again, to do the calculation, the unit-cell dimensions, ion positions, and labeling established by David and coworkers [224] were adopted. Table 9.1 shows this information.

Table 9.1: Crystallographic data for YBCO superconductor at room temperature.

Ions	Wyckoff symbol	x	y	z
Y	1h	1/2	1/2	1/2
Ba	2t	1/2	1/2	0.1844
Cu1	1a	0	0	0
Cu2	2q	0	0	0.3554
O1	1e	0	1/2	0
O2	2s	1/2	0	0.3788
O3	2r	0	1/2	0.3771
O4	2q	0	0	0.1579
	$a = 3.8187$ Å	$b = 3.8833$ Å	$c = 11.6687$ Å	

Source: David and coworkers [224].

For valences, the seven possible copper–oxygen ionic-charge configurations suggested by Müller [239] were used. To deduce these valences, Müller made two assumptions: (1) unit-cell charge neutrality, and (2) oxygen ions possess only -1 or -2 charges. From the measurement results of $\eta_2 \cong 1$ and $\eta_2 \cong 0$, where η_1 and η_2 denote the asymmetry parameters at the Cu1 and Cu2 sites, Müller concluded that O2 and O3 must have the same valences. The nominal charges $+3$ and $+2$ were assigned to yttrium and barium, respectively.

The ion-charge configurations and the site potentials are shown in Table 9.2. For each configuration, Table 9.2 shows also the associated total ionic energy, Madelung constant, and the calculated bulk modulus using the method given in Chapter VI.

As shown in Table 9.2, the Madelung energy depends strongly on ionic-charge configuration and varies over a wide range: from -153 to -336 eV/molecule. The site potentials also change remarkably with ionic charges. In the actual superconductor, $Y_1Ba_2Cu_3O_{7-\delta}$, δ varies between 0 and 0.5. Thus, one of the four oxygen sites is occupied incompletely. This site may be electrostatically unstable, that is, possess the highest potential energy. Beech and coworkers [240] identified this partly occupied site as O1. According to Table 9.2, only ionic-charge configurations I and III have a high potential energy at the O1 site. In these two configurations, the site potential for Cu2 exhibits a big difference: -4 eV in I and -50 eV in III, that is, Cu2 is much more stable in III than in I. Therefore, the two possibilities can be distinguished by the difference of site potential for Cu2 in the configurations I and III.

The possibilities of configurations I and III can be also distinguished by considering the bulk moduli: 53 and 113 GPa in I and III, respectively. In this study, the measured-polycrystal bulk modulus is 101 GPa. Using X-ray-diffraction, Aleksandrov and coworkers [173] found for monocrystal $B = 115$ GPa. Thus, the observed bulk modulus supports strongly charge configuration III.

Since no one reported evidence for a valence of +3 at the Cu2 site, a perturbation of configuration III is proposed. The results are shown in Table 9.2 as configuration A. Obviously, configuration A can be also considered as a perturbation of configurations V and VII. In configuration A, the valences for Cu1 and Cu2 are equalized as +2, the usual oxidation state. Also, one hole was introduced into the CuO_2 plane, on the oxygen sites. Followed Müller's idea [239], we assumed that the hole was equally distributed at the two oxygen sites O2 and O3. We think that superconductivity in YBCO arises from hole pairs in the CuO_2 planes. In configuration A, compared with configuration III, even though the site potential of O1 was remarkably decreased, O1 remains the most unstable site among the oxygen sites. The bulk modulus was reduced only slightly: from 113 to 98 GPa.

Table 9.2: Site potentials and Madelung energies in YBCO for various ion-charge configurations.

	Configuration							
	I	II	III	IV	V	VI	VII	A
Valence								
Cu1	1	1	1	2	2	3	3	2
Cu2	1	2	3	1	2	1	2	2
O1	−2	−2	−2	−1	−1	−2	−2	−2
O2	−1	−2	−2	−2	−2	−2	−2	−1.75
O3	−1	−2	−2	−2	−2	−2	−2	−1.75
O4	−2	−1	−2	−1	−2	−1	−2	−2
Site potential Φ_i *(eV)*								
Y	−31.22	−89.31	−50.29	−138.87	−99.84	−138.88	−99.85	−70.30
Ba	−48.52	−34.75	−46.78	−21.93	−33.95	−22.57	−34.59	−41.12
Cu1	−35.05	−17.76	−33.26	−8.24	−39.26	−43.03	−89.55	−64.01
Cu2	−3.89	−49.94	−76.39	−28.42	−57.83	−28.40	−57.79	−43.57
O1	−2.39	−32.55	−5.79	−29.95	−16.57	−80.34	−53.59	−28.84
O2	−23.95	−45.04	−68.47	−14.52	−37.95	−14.54	−37.98	−42.07
O3	−23.88	−44.82	−67.63	−14.90	−37.81	−14.87	−37.78	−41.80
O4	−18.39	−10.51	−23.56	−21.01	−44.56	−22.10	−46.73	−33.85
Total ionic energy (eV/molecule)	−152.96	−254.87	−327.60	−189.31	−289.94	−233.61	−336.36	−283.98
Total ionic energy (MJ/mol)	−14.76	−24.59	−31.61	−18.26	−27.97	−22.54	−32.45	−27.40
Madelung constant	40.56	67.59	86.88	50.20	76.89	61.95	89.20	75.31
Bulk modulus (GPa)	52.72	87.84	112.91	65.25	99.93	80.51	115.92	97.87

Chapter 10

Calculated Pressure Derivative and Uniaxial-stress Derivatives of T_C

The critical-temperature pressure derivative dT_c/dP plays a central role in the thermodynamics of superconductors [241].

In nontransition-metal conventional superconductors, dT_c/dP is usually negative because pressure increases the elastic stiffness, the Debye temperature, and the average phonon frequency. In transition-metal conventional superconductors, dT_c/dP may be negative or positive because of a competing effect: the increase in T_c from an increase in the ionic potential [242].

For $Y_1Ba_2Cu_3O_{7-\delta}$, reported dT_c/dP values range from -0.8 to 4.3 K/GPa [243,244]. The $dT_c/d\sigma_{ij}$ values disagree even more [110,183,245–247]. Therefore, an estimate of dT_c/dP based on theory might reduce the uncertainty in dT_c/dP.

As described in Chapter IX, the ionic model has been successfully used to describe the charge distributions in YBCO metal-oxide superconductor. Besides the charge distributions, Ohta and coworkers [248] used an ionic model to study the dependence of T_c on the Madelung site potential. Defining ΔV_A as the difference in Madelung site potentials for a hole between the apex and in-plane oxygens (in David's notation, O4 and O2,O3, respectively), they found a remarkable correlation between T_c and ΔV_A, shown in Fig. 10.1, for all known metal-oxide superconductors. The compounds shown in Fig. 10.1 can be identified in Table 10.1, which shows the names, T_c, and calculated

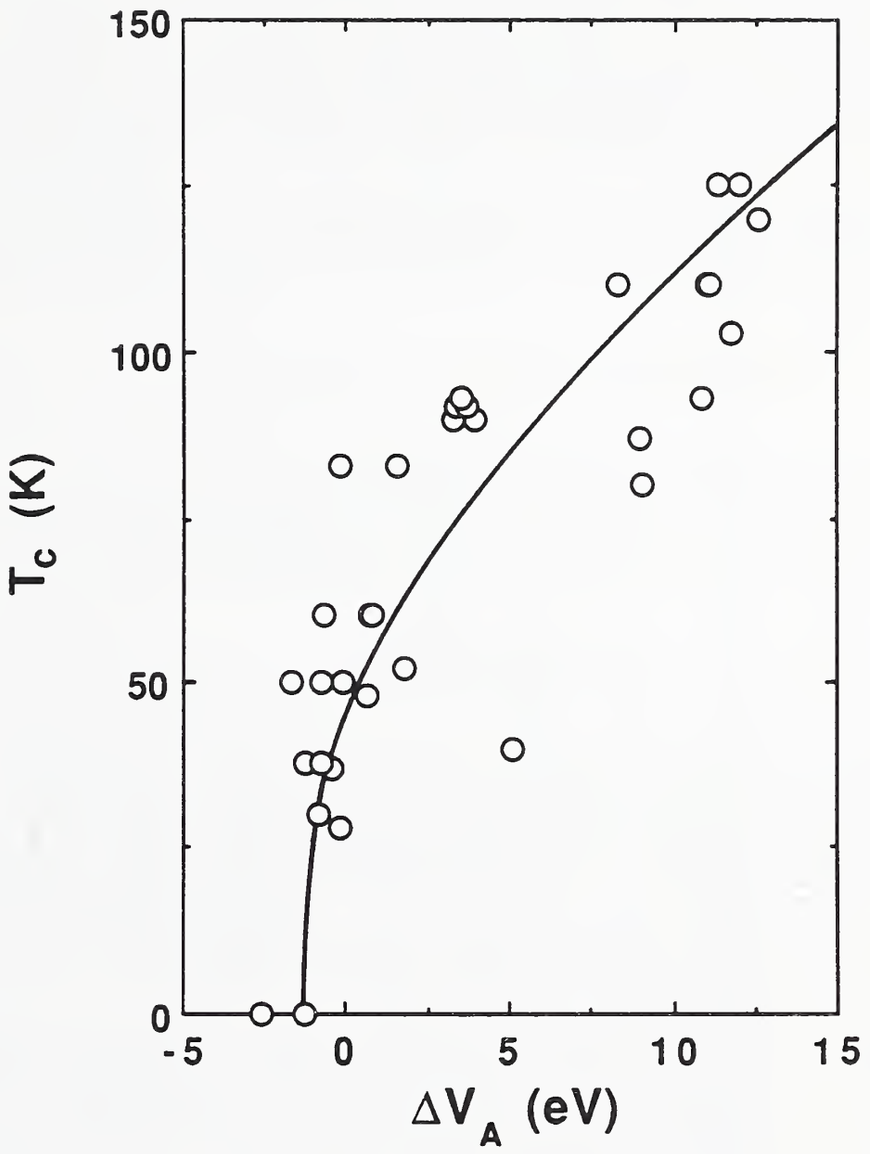

Figure 10.1: T_c-versus-ΔV_A correlation.

ΔV_A of the compounds. From the curve, they concluded that ΔV_A governs T_c in hole-carrier superconductors. They also explained in terms of the T_c–ΔV_A curve why the pressure coefficient dT_c/dP should be proportional to the gradient $dT_c/d\Delta V_A$ of the T_c–ΔV_A curve. In this chapter, the T_c–ΔV_A correlation will be used to calculate the pressure derivative coefficient dT_c/dP and the three principal uniaxial-stress derivatives $dT_c/d\sigma_a$, $dT_c/d\sigma_b$, and $dT_c/d\sigma_c$ for YBCO.

To use Ohta's correlation, an analytic expression for the T_c–ΔV_A relation is needed. Using a least-squares fit, we obtain an empirical expression for T_c in terms of ΔV_A:

$$T_c = 10.57 + 30.25\,(1.43 + \Delta V_A)^{1/2}\,, \tag{10.1}$$

where the units are in K for T_c and eV for ΔV_A.

The site potential for a hole at the position of ith ion V_i (the electrostatic energy to bring a hole from infinity to the i-site) is defined by

$$V_i = \sum_{j \neq i} \frac{Z_j e^2}{\mid \vec{r_j} - \vec{r_i} \mid}. \tag{10.2}$$

Here, $\vec{r_j}$ denotes the position of jth ion, and $Z_j e$ the associated charge. Again, it is assumed that the total charge of the lattice is neutral: $\sum_j Z_j = 0$. The ionic charges were assigned to each individual ion as +3 for Y, +2 for Ba, +3 for Cu1, +2 for Cu2, and −2 for O1−O4. An average potential of O2 and O3 sites was taken to be the in-plane oxygen site potential. The values for O2 and O3 sites differ only by about 0.5%.

To evaluate the site-potential change under certain pressure (or stress), we need to know how the corresponding unit-cell dimensions change (assuming the ions inside the unit cell will change homogeneously), hence the information about the strain. This leads to a need for the elastic constants. Since no measured monocrystal elastic constants as a full set (nine for orthorhombic phase) for YBCO are available, the estimated values for C_{ij} were used (see Table 7.1). The unit-cell dimensions and ionic coordinates of David and coworkers [224] were used for the Madelung-site-potential calculations.

Table 10.2 shows the results for a pressure, and for compressive uniaxial stresses, of 0.5 GPa. Values calculated for lower pressure or stress differ up to a few percent. Values for higher pressure or stress differ similarly, but may

Table 10.1: Transition temperature T_c and ΔV_A for metal-oxide superconductors.

Compounds	T_c (K)	ΔV_A (eV)
$La_2SrCu_2O_{6.2}$	0	−2.639
$La_{1.9}Ca_{1.1}Cu_2O_6$	0	−1.316
$La_{1.85}Sr_{0.15}CuO_4$(I)	38	−0.750
$La_{1.85}Sr_{0.15}CuO_4$(II)	38	−1.267
$La_{1.85}Ba_{0.15}CuO_4$	30	−0.861
$Nd_{1.66}Sr_{0.205}Ce_{0.135}CuO_4$	28	−0.224
$SmLa_{0.75}Sr_{0.25}CuO_{3.95}$	37	−0.463
$(Ba_{0.67}Eu_{0.33})_2(Eu_{0.67}Ce_{0.33})_2Cu_3O_{8+z}$	48	0.630
$Y_{0.8}Ca_{0.2}Ba_2Cu_3O_{6.11}$(I)	50	−0.141
$Y_{0.8}Ca_{0.2}Ba_2Cu_3O_{6.11}$(II)	50	−1.691
$Y_{0.8}Ca_{0.2}Ba_2Cu_3O_{6.11}$(III)	50	−0.770
$YBa_2Cu_3O_{6.5}$	60	0.815
$YBa_2Cu_3O_7$	93	3.533
$ErBa_2Cu_3O_{6.53}$(I)	60	−0.698
$ErBa_2Cu_3O_{6.53}$(II)	60	0.716
$ErBa_2Cu_3O_7$	92	3.679
$Y_{0.9}Ca_{0.1}Ba_2Cu_4O_8$(I)	90	3.244
$Y_{0.9}Ca_{0.1}Ba_2Cu_4O_8$(II)	92	3.362
$(Ca_{0.5}La_{0.5})(Ba_{1.25}La_{0.75})Cu_3O_{6+\delta}$	90	3.896
$Pb_2Sr_2Y_{0.5}Ca_{0.5}Cu_3O_8$(I)	83	−0.242
$Pb_2Sr_2Y_{0.5}Ca_{0.5}Cu_3O_8$(II)	83	1.560
$Pb_{0.5}Tl_{0.5}Sr_2CaCu_2O_7$	110	11.033
$Pb_{0.5}Tl_{0.5}Sr_2Ca_2Cu_3O_9$	125	12.008
$Tl(Ba_{0.6}La_{0.4})_2CuO_{5-\delta}$	52	1.739
$TlBa_2CaCu_2O_{7-\delta}$	103	11.812
$TlBa_2Ca_2Cu_3O_{9-\delta}$	120	12.584
$Tl_2Ba_2CuO_6$	87	8.942
$Tl_2Ba_2CaCu_2O_8$	110	11.112
$Tl_2Ba_2Ca_2Cu_3O_{10}$	125	11.346
$Bi_2Sr_2CuO_{6+\delta}$	80	9.088
$Bi_2Sr_2Ca_{0.9}Y_{0.1}Cu_2O_{8.24}$	93	10.901
$Bi_2Sr_2Ca_2Cu_3O_{10+\delta}$	110	8.300
$Bi_2Sr_2(Gd_{0.82}Ce_{0.18})_2Cu_2O_{10.24}$	40	5.056

Table 10.2: Estimated pressure (stress) and strain derivatives of T_c for YBCO superconductor.

	a	b	c	Hydrostatic
$dT_c/d\sigma_{ij}$ (K/GPa)	0.093	−0.063	0.102	0.093
$dT_c/d\varepsilon_{ij}$ (K)	23.3	−6.9	12.2	–

Note that throughout this chapter, against usual convention, a compressive stress is considered positive. This facilitates easy comparison between pressure and stress effect.

lack meaning because high pressure may change the relative ion positions within the unit cell.

Compared with measurements [243, 244], which range from negative values to 4.3 K/GPa, the result for dT_c/dP falls among the lower positive values. This can be interpreted as follows. This calculation was based on a high-oxygen-content material: $Y_1Ba_2Cu_3O_{6.85}$. Several authors [242, 243] showed that dT_c/dp tends to decrease with increasing T_c and probably approaches zero when T_c becomes about 100 K or when $(b-a)/a$ reaches 0.018 [244]. All this emphasizes the role of oxygen content and oxygen atom positions in affecting both T_c and dT_c/dP. We conjecture that the effect of pressure is to place oxygen atoms in positions more favorable for high T_c. But, in high-oxygen-content materials (near O_7) pressure produces little effect and may decrease T_c.

The anisotropy in $dT_c/d\sigma_{ij}$ is interesting: $dT_c/d\sigma_c \approx dT_c/d\sigma_a$, but $dT_c/d\sigma_b$ negative. Contrary to expectation, compression along the c-axis, which pushes the CuO_2 planes together, fails to increase T_c significantly more than compression along the a-axis, which pulls them apart through a Poisson effect. The negative $dT_c/d\sigma_b$ value agrees with results derived from neutron-diffraction studies by Millis and Rabe [183]. All three predicted $dT_c/d\sigma_{ij}$ are consistent with increasing b unit-cell dimension resulting higher T_c. The increase of T_c with increasing b is well established in many studies, for example Cava and coworkers [249].

Table 10.3: For YBCO, estimated plane-stress and plane-strain derivatives of T_c.

	a–b	a–c
$dT_c/d\sigma_{ij}$ (K/GPa)	0.04	0.17
$dT_c/d\varepsilon_{ij}$ (K)	17.24	35.00

Table 10.2 shows also the strain derivatives $dT_c/d\varepsilon_{ij}$ for the three principal axes. The uniaxial strain applied to each principal axis was 3%. These derivatives avoid knowing the elastic constants C_{ij}, and they represent more fundamental properties. The results show the largest effect on T_c associated with compressing the a-axis. They confirm that a compressive strain along the c-axis produces nothing remarkable and that a strain along the b-axis lowers T_c.

Because both a-axis and c-axis compressions increase T_c, the effect of plane stress and plane strain in the a–c plane should be considered. Table 10.3 shows the results together with those for the a–b plane. As expected, compressing the a–c plane gives a large effect, about twice that of hydrostatic pressure.

Chapter 11

Summary and Conclusions

The elastic and related properties of some oxides and high-T_c oxide superconductors were studied using both measurements and modeling. The physical parameters considered in this study include longitudinal and shear sound velocities v_ℓ and v_t; mass density ρ; elastic moduli B, E, G and Poisson ratio ν of polycrystals, especially the bulk modulus B; elastic stiffnesses C_{ij} of monocrystals; atomic volume V_a; Einstein temperature Θ_E; Debye temperature Θ_D; Grüneisen parameter γ; electron–phonon interaction parameter λ; Madelung energy E_M and site potential Φ_i; critical superconducting transition temperature T_c; ionic charge Z_i; and pressure derivative, dT_c/dP, stress derivative, $dT_c/d\sigma_{ij}$, and strain derivative, $dT_c/d\varepsilon_{ij}$. For three oxides—$BaTiO_3$, $SrTiO_3$, YBCO—elastic constants were measured between 295 and 4 K.

The present study led to ten conclusions:

1. Using a megahertz-frequency pulse-echo method, the intrinsic elastic constants of monocrystalline $SrTiO_3$ and polycrystalline YBCO at room temperature were determined. The measurements for $SrTiO_3$ agree well with those reported by Bell and coworkers and Wachtman and coworkers. The results for YBCO were corrected to the void-free state using a model for a composite material containing spherical particles. The measured bulk modulus $B = 101$ GPa agrees well with the monocrystal measurement, 115 GPa, from a high-pressure X-ray-diffraction study by Aleksandrov and coworkers. Compared with $BaTiO_3$ and $SrTiO_3$, its perovskite-crystal-structure building blocks, YBCO is elastically softer. For example, the bulk modulus equals 101 versus 167 and 180 GPa.

2. The elastic constants of YBCO show different temperature dependences from that of the perovskites, especially $SrTiO_3$. Unlike LSCO and the A15 superconductors, YBCO fails to show elastic-stiffness softening during cooling. Such softening represents a zone-center soft lattice-vibration mode, which many consider related strongly to superconductivity.

3. For the polycrystalline YBCO specimen used in this study, the elastic-modulus–temperature behavior is nearly regular. It fits the Varshni function:

$$C_T = C_0 - \frac{s}{\exp(\Theta_E/T) - 1}.$$

Here, C_0 denotes an elastic constant at $T = 0$ K, Θ_E the Einstein temperature, and s a parameter that relates to zero-point vibrations and can be calculated from Θ_E, V_a, and γ. Contrary to many other reports, this specimen showed practically no C_T hysteresis. The Poisson ratio provides an exception to the regular (Einstein-model) temperature-dependent behavior. Near T_c, rather than decreasing smoothly during cooling, the Poisson ratio shows an anomalous drop, which reflects some internal change in YBCO.

4. Within measurement error, about 5 in 10^4, and contrary to many other reports, the elastic stiffnesses showed no change near T_c during cooling. This agrees with the small thermodynamically predicted change: about 1 in 10^5.

5. The bulk modulus of YBCO was calculated using a Born ionic model, which contains only two terms: Madelung energy and ion-core repulsion energy. The calculation supports the measurement result. This indicates that covalent forces are weak compared with ionic interactions and that metallic bonding makes no large contribution to the bulk modulus.

6. From the measured polycrystal elastic constants of YBCO, the Debye characteristic temperature was determined. The result, $\Theta_D^0 = 437$ K, agrees well with the specific-heat value, 440 K. The temperature dependences of the Debye temperatures were determined also. The results showed that $BaTiO_3$, $SrTiO_3$, and YBCO show different temperature dependences. Thus, these oxides show no common C_T behavior.

7. For orthorhombic YBCO, nine independent elastic stiffnesses C_{ij} were estimated based on monocrystal measurements combined with analysis–theory. The results are shown in Table 7.1. The Debye temperature and the bulk modulus calculated from the estimated C_{ij} agree with the corresponding values determined from specific-heat measurement and a high-pressure X-ray-diffraction study.

8. For several oxide superconductors, the electron–phonon parameters λ were calculated from T_c and Θ_D^0 using Kresin's model, which is valid for all values of λ. For YBCO, $\lambda = 2.24$. This realistic λ value allows for a possible BCS superconductivity mechanism. The calculations indicate that a stronger electron–phonon interaction yields a higher superconducting transition temperature.

9. By Ewald's method, the ion-site potentials and Madelung energy were calculated to determine the possible valence configuration for $Y_1Ba_2Cu_3O_7$. Among seven suggested possibilities, only one ion-charge configuration allows for vacancies at the O1 site and also gives a realistic bulk modulus. A perturbation of this configuration by equalizing the Cu1–Cu2 charges as +2 and introducing a hole into the CuO_2 plane at the oxygen sites also gives reasonable agreement with observation.

10. By calculating the Madelung site potentials and using the estimated C_{ij}, we determined the difference in Madelung site potentials for a hole at the apical and planar oxygens ΔV_A for hydrostatic pressure, compressive stresses, and compressive strains. Applying Ohta's relationship for T_c and ΔV_A, the pressure derivative dT_c/dP, uniaxial-stress and plane-stress derivatives $dT_c/d\sigma_{ij}$, and uniaxial-strain and plane-strain derivatives $dT_c/d\varepsilon_{ij}$ were calculated. The results show that T_c increases with decreasing both a and c axes and with increasing b-axis. This is consistent with the current view that T_c increases as the c-axis decreases, as the CuO_2 planes move closer together. The results show also that compressing the a–c plane increases T_c the most, about twice that of hydrostatic pressure. These calculations imply several possibilities for increasing T_c.

Acknowledgments

This publication represents the thesis submitted by Ming Lei to the University of Colorado (Boulder) to satisfy part of the requirements for the Ph.D. degree. Dr. Ledbetter directed the thesis research.

The authors thank S. Kim at NIST for his assistance with measurements and Dr. Z. Sheng at University of Arkansas for supplying the YBCO specimen. Critical readings were provided by Professors S. Datta, A. Hermann, J. Scott, and P. Zoller at the University of Colorado.

References

[1] H.M. Ledbetter, "Elastic properties," in *Materials at Low Temperatures* (Amer. Soc. Met., Metals Park, 1983), p. 1.

[2] D.C. Wallace, *Thermodynamics of Crystals* (Wiley, New York, 1972), p. 102.

[3] H.K. Kamerlingh-Onnes, "Further experiments with liquid helium. D. On the change of the electrical resistence of pure metals at very low temperatures, etc. V. The disappearance of the resistance of mercury," Akad. Wetenschappen (Amsterdam) **14**, 113 (1911).

[4] J. Bardeen, L.N. Cooper, J.R. Schrieffer, "Theory of superconductivity," Phys. Rev. **108**, 1175 (1957).

[5] M. Blackman, "The specific heat of solids," in *Handbuch der Physik* (Springer, Berlin, 1955), Vol. **7**, Part I, p. 325.

[6] G. Grimvall, *The Electron–Phonon Interaction in Metals* (North-Holland, Amsterdam, 1981), p. 3.

[7] W.L. Bond, W.P. Mason, and H.J. McSkimin, "Elastic and electromechanical coupling coefficients of single-crystal barium titanate," Phys. Rev. **82**, 442 (1951).

[8] R. Bechmann, "Elastic, piezoelectric, and dielectric constants of polarized barium titanate ceramics and some applications of the piezoelectric equations," J. Acoust. Soc. Am. **28**, 347 (1956).

[9] D. Berlincourt and H. Jaffe, "Elastic and piezoelectric coefficients of single-crystal barium titanate," Phys. Rev. **111**, 143 (1958).

[10] E.J. Huibregtse, W.H. Bessey, and M.E. Drougard, "Electromechanical behavior of single crystals of barium titanate from 25 to 160°C," J. Appl. Phys. **30**, 899 (1959).

[11] S. Fushimi and T. Ikeda, "Elastic properties of barium titanate single crystal above the Curie point," Rev. Electr. Commun. Lab. **14**, 161 (1966).

[12] B.A. Strukov and K.V. Garland, "Ultrasonic relaxation in $BaTiO_3$ crystals close to the Curie point," Sov. Phys. Crystallogr. **19**, 175 (1974).

[13] G. Mader, H. Meixner, and P. Kleinschmidt, "Temperature and stress dependence of Young's modulus in semiconducting barium titanate ceramics," J. Appl. Phys. **58**, 702 (1985).

[14] I.T. Perro and V.Y. Fritsberg, "Singularities of the elastic properties of barium titanate due to structural changes near the tetragonal-cubic phase transition," Sov. Phys. Solid State **21**, 1832 (1979).

[15] H. Beige and G. Schmidt, "Resonant determination of high-order elastic coefficients and the elastic nonlinearity of a paraelectric ferroelectric," Izv. Akad. Nauk. SSSR Ser. Fiz. **39**, 970 (1975).

[16] A.A. Demidenko, A.P. Zdebskii, V.N. Piskovoi, and A.V. Savchuk, "Determination of nonlinear elastic coefficients by resonant methods," Phys. Stat. Sol. (a) **79**, K73 (1983).

[17] A. Schaefer, H. Schmitt, and A. Dörr, "Elastic and piezoelectric coefficients of TSSG barium titanate single crystals," Ferroelectrics **69**, 253 (1986).

[18] A.F. Devonshire, "Theory of barium titanate.—Part I," Phil. Mag. **40**, 1040 (1949); "Theory of barium titanate.—Part II," Phil. Mag. **42**, 1065 (1951).

[19] A.V. Turik, "Elastic, piezoelectric, and dielectric properties of single crystals of $BaTiO_3$ with a laminar domain structure," Sov. Phys. Solid State **12**, 688 (1970).

[20] S. Yokoyama, K.N. Pak, and W. Kinase, "Elastic compliances of barium titanate crystal," Phys. Lett. **46A**, 305 (1974).

[21] H. Beige, "Nonlinear properties of paraelectric barium titanate crystals," Acta Phys. Slov. **30**, 71 (1980).

[22] D. Jannot, C. Escribe-Filippini, and J. Bouillot, "Lattice dynamics of pure barium titanate and barium strontium titanate solid solutions," J.Phys. C: Solid State Phys. **17**, 1329 (1984).

[23] J.F. Scott, "Soft-mode spectroscopy: Experimental studies of structural phase transitions," Rev. Mod. Phys. **46**, 83 (1974).

[24] E. Poindexter and A.A. Giardini, "Elastic constants of strontium titanate ($SrTiO_3$)," Phys. Rev. **110**, 1069 (1958).

[25] R.O. Bell and G. Rupprecht, "Elastic constants of strontium titanate," Phys. Rev. **129**, 90 (1963).

[26] J.B. Wachtman, M.L. Wheat, and S. Marzullo, "A method for determining the elastic constants of a cubic crystal from velocity measurements in a single arbitrary direction; Application to $SrTiO_3$," J. Res. Nat. Bur. Stand. (U.S.) **67A**, 193 (1963).

[27] G. Rupprecht and W.H. Winter, "Electromechanical behavior of single-crystal strontium titanate," Phys. Rev. **155**, 1019 (1967).

[28] G. Sorge and E. Hegenbarth, "The temperature dependence of the elastic compliance S_{11}^E of $SrTiO_3$ single crystals in the temperature range 20 to 45° K," Phys. Status Solidi **33**, K79 (1969).

[29] J.E. Mackey and R.T. Arnold, "Some combinations of third-order elastic constants for strontium titanate single crystals," J. Appl. Phys. **40**, 4806 (1969).

[30] E.L. Meeks and R.T. Arnold, "Temperature dependence of the third-order elastic constants of $SrTiO_3$," Phys. Rev. B **1**, 982 (1970).

[31] B. Lüthi and T.J. Moran, "Sound propagation near the structural phase transition in strontium titanate," Phys. Rev. B **2**, 1211 (1970).

[32] A.G. Beattie and G.A. Samara, "Pressure dependence of the elastic constants of $SrTiO_3$," J. Appl. Phys. **42**, 2376 (1971).

[33] R.D. Peters and R.T. Arnold, "Ultrasonic third-harmonic generation in strontium titanate single crystals," J. Appl. Phys. **42**, 980 (1971).

[34] K. Fossheim and B. Berre, "Ultrasonic propagation, stress effects, and interaction parameters at the displacive transition in $SrTiO_3$," Phys. Rev. B **5**, 3292 (1972).

[35] W. Rehwald, "Low temperature elastic moduli of strontium titanate," Solid State Commun. **8**, 1483 (1970).

[36] W. Rehwald, "Critical behavior of strontium titanate under stress," Solid State Commun. **21**, 667 (1977).

[37] U.T. Höchli and A.D. Bruce, "Elastic critical behaviour in $SrTiO_3$," J. Phys. C: Solid State Phys. **13**, 1963 (1980).

[38] B.N.N. Achar, G.R. Barsch, and L.E. Cross, "Static shell model calculation of electrostriction and third order elastic coefficients of perovskite oxides," Ferroelectrics **37**, 495 (1981).

[39] B.N.N. Achar, G.R. Barsch, and L.E. Cross, "Electrostriction, optic mode γ's, and third-order elastic constants of $SrTiO_3$ in the shell model," Phys. Rev. B **24**, 1029 (1981).

[40] D.Y. Chung and Y. Li, "The determination of elastic constants using arbitrary directions in cubic and hexagonal crystals," Phys. Lett. **58A**, 133 (1976).

[41] J.F. Schooley, W.R. Hosler, and M.L. Cohen, "Superconductivity in semiconducting $SrTiO_3$," Phys. Rev. Lett. **12**, 474 (1964).

[42] A.W. Sleight, J.L. Gillson, and P.E. Bierstedt, "High-temperature superconductivity in the $BaPb_{1-x}Bi_xO_3$ system," Solid State Commun. **17**, 27 (1975).

[43] J.G. Bednorz and K.A. Müller, "Possible high-T_c superconductivity in the Ba-La-Cu-O system," Z. Phys. B **64**, 189 (1986).

[44] M.K. Wu, J.R. Ashburn, C.J. Torng, P.H. Hor, R.L. Meng, L. Gao, Z.J. Hwang, Y.Q. Wang, and C.W. Chu, "Superconductivity at 93 K in a new mixed-phase Y-Ba-Cu-O compound system at ambient pressure," Phys. Rev. Lett. **58**, 908 (1987).

[45] H.M. Ledbetter, "Elastic properties of metal-oxide superconductors," J. Metals **40**, 24 (1988).

[46] D.R. Lundy, L.J. Swartzendruber, and L.H. Bennett, "A brief review of recent superconductivity research at NIST," J. Res. Nat. Inst. Stand. Tech. **94**, 147 (1989).

[47] J. Dominec, "Sound attenuation and velocity in superconductive ceramics—a review," Supercond. Sci. Technol. **2**, 91 (1989).

[48] R. Srinivasan, "Sound velocity and elastic constants in oxide superconductors," in *Studies of High Temperature Superconductors* (Nova, Commack, New York, 1989), Vol. **1**, p. 267.

[49] K. Fossheim and T. Lægreid, "A review of elastic properties of high-T_c superconductors and some related C_p results," IBM J. Res. Develop. **33**, 365 (1989).

[50] T. Lægreid, K. Fossheim, S. Sathish, F. Vassenden, O. Traetteberg, E. Sandvold, and T. Bye, "Elastic and thermodynamic properties of high temperature superconductors, a brief review," Physica Scripta **T23**, 116 (1988).

[51] H.M. Ledbetter, M.W. Austin, S.A. Kim, and Ming Lei, "Elastic constants and Debye temperature of polycrystalline $Y_1Ba_2Cu_3O_{7-x}$," J. Mater. Res. **2**, 786 (1987).

[52] S. Block, G.J. Piermarini, R.G. Munro, and W. Wong-Ng, "The bulk modulus and Young's modulus of the superconductor $Y_1Ba_2Cu_3O_7$," Adv. Ceram. Mater. **2** Special Issue 3B, 601 (1987).

[53] D.P. Almond, E. Lambson, G.A. Saunders, and Wang Hong, "An ultrasonic study of the elastic properties of the normal and superconducting states of $YBa_2Cu_3O_{7-\delta}$," J. Phys. F: Met. Phys. **17**, L221 (1987).

[54] H.M. Ledbetter, M.W. Austin, S.A. Kim, T. Datta, and C.E. Violet, "Shear-modulus change below T_c in $YBa_2Cu_3O_{7-x}$," J. Mater. Res. **2**, 790 (1987).

[55] D.P. Almond, E.F. Lambson, G.A. Saunders, and Wang Hong, "Ultrasonic attenuation in the high-T_c superconductor $YBa_2Cu_3O_{7-\delta}$," J. Phys. F: Met. Phys. **17**, L261 (1987).

[56] S. Bhattacharya, M.J. Higgins, D.C. Johnson, A.J. Jacobson, J.P. Stokes, J.T. Lewandowski, and D.P. Goshorn, "Anomalous ultrasound propagation in high-T_c superconductors: $La_{1.8}Sr_{0.2}CuO_{4-y}$ and $YBa_2Cu_3O_{7-\delta}$," Phys. Rev. B **37**, 5901 (1988).

[57] S. Ewert, S. Guo, P. Lemmens, F. Stellmach, J. Wynants, G. Arlt, Dorothee Bonnenberg, H. Kliem, A. Comberg, and H. Passing, "Ultrasonic investigations on superconducting $YBa_2Cu_3O_{7-\delta}$ samples of different microstructure," Solid State Commun. **64**, 1153 (1987).

[58] Y. Horie, Y. Terashi, H. Fukuda, T. Fukami, and S. Mase, "Ultrasonic studies of the high T_c superconductor $Y_2Ba_4Cu_6O_{14}$," Solid State Commun. **64**, 501 (1987).

[59] T. Lægreid, K. Fossheim, and F. Vassenden, "Elastic and thermal behaviour of ceramic high-T_c superconductors studied by ultrasound, vibrating reed, and specific heat measurements," Physica C **153–155**, 1096 (1988).

[60] P. Lemmens, F. Stellmach, S. Ewert, S. Guo, J. Wynants, G. Arlt, A. Comberg, H. Passing, and G. Marbach, "Ultrasound study of $YBa_2Cu_3O_{7-\delta}$ samples of different microstructure," Physics C **153–155**, 294 (1988).

[61] V. Ramachandran, G.A. Ramadass, and R. Srinivasan, "Acoustic wave velocity and attenuation in the high T_c superconductor $YBa_2Cu_3O_7$," Physica C **153–155**, 278 (1988).

[62] N.V. Anshukova, G.P. Vorob'ev, A.I. Golovashkin, O.M. Ivanenko, Z.A. Kazei, I.B. Krynetskii, R.Z. Levitin, B.V. Mil', K.V. Mitsen, and V.V.

Snegirev, "Thermal expansion and elastic properties of the high-temperature superconductors (Y,Ho)$Ba_2Cu_3O_9$," JETP Lett. **46**, 471 (1987).

[63] D.J. Bishop, A.P. Ramirez, P.L. Gammel, B. Batlogg, E.A. Rietman, R.J. Cava, and A.J. Millis, "Bulk-modulus anomalies at the superconducting transition of single-phase $YBa_2Cu_3O_7$," Phys. Rev. B **36**, 2408 (1987).

[64] M. Núñez Requeiro, P. Esquinazi, M.A. Izbizky, C. Durán, D. Castello, J. Luzuriaga, and G. Nieva, "Evidence of tunneling systems through thermal and acoustic measurements in ceramic materials," Physica C **153–155**, 1016 (1988).

[65] M. Suzuki, Y. Okuda, I. Iwasa, A.J. Ikushima, T. Takabatake, Y. Nakazawa, and M. Ishikawa, "Ultrasonic studies of the high-T_c superconductor $YBa_2Cu_3O_y$," Jpn. J. Appl. Phys. Suppl. **27**, L308 (1988).

[66] M. Suzuki, Y. Okuda, I. Iwasa, A.J. Ikushima, T. Takabatake, Y. Nakazawa, and M. Ishikawa, "Sound velocity anomaly of $YBa_2Cu_3O_y$," Physica C **153–155**, 266 (1988).

[67] B. Wolf, T.J. Kim, H. Kühnberger. W. Palme, A. Krimmel, I. Zanthopoulos, W. Grill, and B. Lüthi, "Ultrasonic and high magnetic field properties of $YBa_2Cu_3O_{7-\delta}$," Physica C **153–155**, 284 (1988).

[68] A.I. Golovashkin, V.A. Danilov, O.M. Ivanenko, G.M. Leitus, K.V. Mitsen, I.I. Perepechko, O.G. Karpinskii, and V.F. Shamray, "Anomalous behavior of the elastic characteristics of $YBa_2Cu_3O_7$ near T_c," in *Novel Superconductivity* (Plenum, New York, 1987), p. 883.

[69] A.I. Golovashkin, V.A. Danilov, O.M. Ivanenko, K.V. Mitsen, and I.I. Perepechko, "Anomalies in the velocity of sound and in the elastic moduli near the superconducting transition of the ceramic $YBa_2Cu_3O_7$," JETP Lett. **46**, 343 (1987).

[70] D.F. Lee and K. Salama, "Elastic properties and Debye characteristic temperature of partially melted $YBa_2Cu_3O_{7-x}$ superconductor," Modern Phys. Lett. B **2**, 1111 (1988).

[71] M.P. Staines, J.L. Tallon, W.H. Robinson, and N.E. Flower, "Atmosphere-sensitive 225 K feature in interal friction of $YBa_2Cu_3O_{7-\delta}$," Appl. Phys. Lett. **53**, 1560 (1988).

[72] J.L. Tallon, A.H. Schuitema, and N.E. Tapp, "Soft mode behavior in the orthorhombic to tetragonal transition in the high T_c superconductor $YBa_2Cu_3O_{7-\delta}$," Appl. Phys. Lett. **52**, 507 (1988).

[73] R. Calemczuk, E. Bonjour, J.Y. Henry, L. Forro, C. Ayache, M.J.M. Jurgens, J. Rossat-Mignod, B. Barbara, P. Burlet, M. Couach, A.F. Khoder, and B. Salce, "Evidence of a first order phase transition in $YBa_2Cu_3O_{6.9}$ at $T = 230$ K," Physica C **153–155**, 960 (1988).

[74] J.L. Tallon and M.P. Staines, "Elastic properties of $YBa_2Cu_3O_{7-\delta}$," in *High-Temperature Superconductors II* (Mater. Res. Soc., Pittsburgh, 1988), paper K8.32.

[75] Y. Wang, H. Shen, J. Zhu, Z. Xu, M. Gu, Z. Niu, and Z. Zhang, "Study on the anomalies of $YBa_2Cu_3O_{9-x}$ between 90–260 K by elasticity measurements and x-ray diffraction," J. Phys. C: Solid State Phys. **20**, L665 (1987).

[76] A. Migliori, T. Chen, B. Alavi, and G. Grüner, "Ultrasound anomaly at T_c in $YBa_2Cu_3O_y$," Solid State Commun. **63**, 827 (1987).

[77] M. Yoshimoto, S. Tanabe, and N. Soga, "Temperature dependence of elastic properties of $YBa_2Cu_3O_{7-x}$ superconductor," Chem. Lett. **16**, 2193 (1987).

[78] T.J. Kim, B. Lüthi, M. Schwarz, H. Kühnberger, B. Wolf, G. Hampel, D. Nikl, and W. Grill, "Valence fluctuation aspects of high temperature superconductors," J. Magn. Magn. Mater. **76–77**, 604 (1988).

[79] E. Salomons, H. Hemmes, J.J. Scholtz, N. Koeman, R. Brouwer, A. Driessen, D.G. de Groot, and R. Griessen, "Thermal expansion, compressibility and Grüneisen parameter of $YBa_2Cu_3O_x$," Physica **145B**, 253 (1987).

[80] M.R. Dietrich, W.H. Fietz, J. Ecke, and C. Politis, "Structure and superconductivity of $La_{1.8}Sr_{0.2}CuO_4$ and $YBa_2Cu_3O_7$ under high pressure," Jpn. J. Appl. Phys. Suppl. **26–3**, 1113 (1987).

[81] W.H. Fietz, M.R. Dietrich, and J. Ecke, "Possible transformation of $YBa_2Cu_3O_7$ under pressure," Z. Phys. B **69**, 17 (1987).

[82] N.V. Jaya, S. Natarajan, and G.V.S. Rao, "Pressure induced structural phase transition in $YBa_2Cu_3O_7$," Solid State Commun. **67**, 51 (1988).

[83] A. Al-Kheffaji, M. Cankurtaran, G.A. Saunders, D.P. Almond, E.F. Lambson, and R.C. Draper, "Elastic behaviour under pressure of high-T_c superconductors $RBa_2Cu_3O_{7-x}$ (R=Y, Gd and Eu)," Phil. Mag. B **59**, 487 (1989).

[84] M. Cankurtaran, G.A. Saunders, J.R. Willis, A. Al-Kheffaji, and D.P. Almond, "Bulk modulus and its pressure derivative of $YBa_2Cu_3O_{7-x}$," Phys. Rev. B **39**, 2872 (1989).

[85] N.McN. Alford, J.D. Birchall, W.J. Clegg, M.A. Harmer, K. Kendall, and D.H. Jones, "Physical and mechanical properties of $YBa_2Cu_3O_{7-\delta}$ superconductors," J. Mater. Sci. **23**, 761 (1988).

[86] R. Round and B. Bridge, "Elastic constants of the high-temperature ceramic superconductor $YBa_2Cu_3O_{7-x}$," J. Mater. Sci. Lett. **6**, 1471 (1987).

[87] J.W. Severin and G. de With, "Microcracking and mechanical properties of $YBa_2Cu_3O_x$ ceramics," to be published in : Proc. Brit. Ceram. Soc. (1989).

[88] B. Bridge and R. Round, "Density dependence of the ultrasonic properties of high-T_c sintered $YBa_2Cu_3O_{7-x}$ superconductors," J. Mater. Sci. Lett. **8**, 691 (1989).

[89] V.P. Glazkov, I.N. Goncharenko, and V.A. Somenkov, "Neutron diffraction investigation of the compressibility of $YBa_2Cu_3O_{7-x}$ at high pressures," Sov. Phys. Solid State **30**, 2127 (1989).

[90] G.C.S. Chang, S.J. Burns, A. Goyal, and P.D. Funkenbusch, "Young's modulus measurement of polycrystalline $YBa_2Cu_3O_{7-\delta}$ superconductor," in *Ceramic superconductors II* (Westerville, Ohio, 1988), p. 580.

[91] K. Salama, K. Ravi-Chandar, V. Selvamanickam, D.F. Lee, P.K. Reddy, and S.V. Rele, "The influence of fabricating technologies on the structure and properties of $YBa_2Cu_3O_{7-x}$," J. Metals **40(8)**, 6 (1988).

[92] H.M. Ledbetter and S.A. Kim, "Hysteretic phase transition in $Y_1Ba_2Cu_3O_{7-x}$ superconductors," Phys. Rev. B **38**, 11857 (1988).

[93] S. Hoen, L.C. Bourne, C.M. Kim, and A. Zettl, "Elastic response of polycrystalline and single-crystal $YBa_2Cu_3O_7$," Phys. Rev. B **38**, 11949 (1988).

[94] Y. He, B. Zhang, S. Lin, J. Xiang, Y. Lou, and H. Chen, "Ultrasonic investigation of lattice instability and superconductivity in high-T_c systems," J. Phys. F: Met. Phys. **17**, L243 (1987).

[95] M. Lang, T. Lechner, S. Riegel, F. Steglich, G. Weber, T.J. Kim, B. Lüthi, B. Wolf, H. Rietschel, and M. Wilhelm, "Thermal expansion, sound velocities, specific heat and pressure derivative of T_c in $YBa_2Cu_3O_7$," Z. Phys. B **69**, 459 (1988).

[96] Y. Horie, Y. Terashi, and S. Mase, "Ultrasonic studies and phonon modes of $(RE)Ba_2Cu_3O_7$," J. Phys. Soc. Jpn. **58**, 279 (1989).

[97] Y. Horie and S. Mase, "Discontinuity in sound velocity and high T_c superconductivity in $YBa_2Cu_3O_7$," Solid State Commun. **69**, 535 (1989).

[98] P. Lemmens, F. Stellmach, J. Wynants, S. Ewert, A. Comberg, H. Passing, and G. Marbach, "Acoustic measurements on high-T_c superconductors in the systems Y–Ba–Cu–O and Bi,Pb–Sr–Ca–Cu–O," J. Less-Comm. Met. **150**, 1 (1989).

[99] C. Durán, P. Esquinazi, C. Fainstein, and M. Núñez Regueiro, "Anomalies in the internal friction and sound velocity in $YBa_2Cu_3O_{7-x}$

and $EuBa_2Cu_3O_{7-x}$ superconductors," Solid State Commun. **65**, 957 (1988).

[100] S. Bhattacharya, M.J. Higgins, D.C. Johnston, A.J. Jacobson, J.P. Stokes, D.P. Goshorn, and J.T. Lewandowski, "Elastic anomalies and phase transitions in high-T_c superconductors," Phys. Rev. Lett. **60**, 1181 (1988).

[101] P. Esquinazi, C. Durán, C. Fainstein, and M. Núñez Regueiro, "Evidence of low-energy tunneling excitations in the high-T_c superconductor $YBa_2Cu_3O_{7-x}$," Phys. Rev. B **37**, 545 (1988).

[102] J. Du, J. Jiang, X. Wang, and H. Yin, "Studying in-situ on the superconducting transition and internal friction of a high T_c superconductor $YBa_2Cu_3O_{7-\delta}$," Mod. Phys. Lett. B **1**, 425 (1988).

[103] V. Müller and D. Maurer, "Ultrasonic investigations of phase transitions in high-T_c superconductors," Phase Transitions **22**, 211 (1990).

[104] S. Mase, Y. Horie, T. Yasuda, and T. Fukami, "Ultrasonic studies of high T_c ceramic superconductors," in *Ultrasonic Spectroscopy and Its Applications to Materials Science* (Kyushu Univ. Report, Fukuoka, 1987), p. 328.

[105] Y. Horie, Y. Terashi, K. Fukuda, M. Hidaka, T. Fukami, and S. Mase, "Ultrasonic studies of high T_c superconductors," in Proceedings, Second Joint Meeting ASA, ASJ (Nov. 1988).

[106] A.B. Lebedev, Yu.A. Burenkov, V.I. Ivanov, B.K. Kardashev, S.P. Nikanorov, and Yu.P. Stepanov, "Amplitude and temperature dependences of the absorption of ultrasound and of the Young modulus of superconducting ceramic $YBa_2Cu_3O_{7-x}$," Sov. Phys. Solid State **31**, 166 (1989).

[107] V.I. Makarov, N.V. Zavaritskiy, V.S. Klochko, A.P. Voronov, and V.F. Tkachenko, "Acoustic characteristics and structural features of the vibration spectrum of the $La_{2-x}Sr_xCuO_4$ ($x = 0$ and 0.2) lattice and the $YBa_2Cu_3O_y$ ($y = 6$ and 7) lattice," JETP Lett. **48**, 359 (1988).

[108] T. Deng, L. Zhang, H. Gu, Z. Xiao, and L. Chen, "Ultrasonic studies on high T_c superconductor $YBa_2Cu_3O_{7-x}$," Chin. Phys. Lett. **5**, 461 (1988).

[109] M. Saint-Paul, J.L. Tholence, P. Monceau, H. Noel, J.C. Levet, M. Potel, P. Gougeon, and J.J. Capponi, "Ultrasound study of $YBa_2Cu_3O_{7-\delta}$ single crystals," Solid State Commun. **66**, 641 (1988).

[110] X.D. Shi, R.C. Yu, Z.Z. Wang, N.P. Ong, and P.M. Chaikin, "Sound velocity and attenuation in single-crystal $YBa_2Cu_3O_{7-\delta}$," Phys. Rev. B **39**, 827 (1989).

[111] M. Saint-Paul, J.L. Tholence, H. Noël, J.C. Levet, M. Potel, and P. Gougeon, "Ultrasound study on $YBa_2Cu_3O_{7-\delta}$ and $GdBa_2Cu_3O_{7-\delta}$ single crystal," Solid State Commun. **69**, 1161 (1989).

[112] I.V. Aleksandrov, A.F. Goncharov, I.N. Makarenko, A.J. Shapiro, S.M. Stishov, I.P. Zibrov, V.N. Denisov, B.N. Mavrin, V.B. Podobedov, A.P. Volodin, V.A. Melik-Shahchnazarov, and I.I. Mirzoeva, "Systematic study of $YBa_2Cu_3O_x$ single crystal samples at the oxygen content variation," Physica C **162–164**, 1057 (1989).

[113] B. Golding, W.H. Haemmerle, L.F. Schneemeyer, and J.V. Waszczak, "Gigahertz ultrasound in single crystal superconducting $YBa_2Cu_3O_7$," in *IEEE 1988 Ultrasonics Symposium* (IEEE, Piscataway, 1988), p. 1079.

[114] V.A. Melik-Shakhnazarov, I.I. Mirzoeva, T.Sh. Kvirikashvili, S.K. Dzharparidze, I.A. Naskidashvili, I.N. Makarenko, and S.M. Stishov, "Acoustic studies of $YBa_2Cu_3O_x$ single crystals," JETP Lett. **50**, 81 (1989).

[115] A. Zettl, L.C. Bourne, W.N. Creager, M.F. Crommie, and S. Hoen, "Electron–phonon interactions in high-temperature oxide superconductors: isotope effects and elasticity studies," Synthetic Metals **29**, F723 (1989).

[116] B. Lüthi, B. Wolf, T. Kim, W. Grill, and B. Renker, "Sound propagation in high temperature superconductors," Jpn. J. Appl. Phys. Suppl. **26–3**, 1127 (1987).

[117] V. Müller, K. de Groot, D. Maurer, C. Roth, K.H. Rieder, E. Eichenbusch, and R. Schöllhorn, "Sound velocity and ultrasonic absorption in high-T_c-superconductors," Jpn. J. Appl. Phys. Suppl. **26–3**, 2139 (1987).

[118] D.J. Bishop, P.L. Gammel, A.P. Ramirez, B. Batlogg, R.J. Cava, and A.J. Millis, "Bulk modulus anomalies at the superconducting transitions of single-phase $YBa_2Cu_3O_7$ and $La_{1.85}Sr_{0.15}CuO_4$," in *Novel Superconductivity*, ed by S.A. Wolf and V.Z. Kresin (Plenum, New York, 1987), p.659.

[119] B. Golding, N.O. Birge, W.H. Haemmerle, R.J. Cava, and E. Rietman,"Tunneling systems in superconducting $YBa_2Cu_3O_7$," Phys. Rev. B **36**, 5606 (1987).

[120] M.H. Jericho, A.M. Simpson, J.M. Tarascon, L.H. Green, R. McKinnon, and G. Hall, "Thermal expansion and velocity of ultrasonic waves in single phase $YBa_2Cu_3O_{(7-x)}$," Solid State Commun. **65**, 987 (1988).

[121] J. Zhu, Y. Wang, Z. Xu, L. Sun, Y. Rui, M. Gu, H. Shen, and X. Chen, "The effects of thermal cycling from 5 to 350°C on elasticity and superconductivity of $YBa_2Cu_3O_{7-\delta}$," Supercond. Sci. Technol. **1**, 88 (1988).

[122] K. Sun, M. Levy, B.K. Sarma, P.H. Hor, R.L. Meng, Y.Q. Wang, and C.W. Chu, "Ultrasonic measurements on polycrystalline $YBa_2Cu_3O_7$," Phys. Lett. A **131**, 541 (1988).

[123] J. Toulouse, X.M. Wang, and D.J.L. Hong, "Ultrasonic evidence for a structural phase transition at 220 K in $YBa_2Cu_3O_{7-\delta}$," Phys. Rev. B **38**, 7077 (1988).

[124] Z. Zhao, S. Adenwalla, A. Moreau, J.B. Ketterson, Q. Robinson, D.L. Johnson, S.J. Hwu, K.R. Peoppelmeier, M.F. Xu, Y. Hong, R.F. Wiegert, M. Levy, and B.K. Sarma, "Ultrasonic velocity anomalies in superconducting sinter-forged $YBa_2Cu_3O_{7-\delta}$," Phys. Rev. B **39**, 721 (1989).

[125] N.V. Zavaritsky, A.V. Samoilov, A.A. Yurgens, V.S. Klochko, and V.I. Makarov, "Phonon transport phenomena in HTS," M^2S-HTSC Conference (Stanford, July 1989).

[126] L.G. Mamsurova, K.S. Pigalskiy, V.P. Sakun, L.G. Scherbakova, I.E. Graboy, and A.R. Kaul, "Temperature hysteresis of the elastic modulus and low-temperature local phase transformations of the order-disorder type in the superconductor $YBa_2Cu_3O_x$," Phys. Lett. A **131**, 538 (1988).

[127] S. Mase and Y. Horie, "Ultrasonic studies of the roles of electron−phonon interaction in high T_c superconductors," in Proceedings, Second Joint Meeting ASA, ASJ (Nov. 1988).

[128] J.X. Zhang, G.M. Lin, W.G. Zeng, K.F. Liang, Z.C. Lin, G.G. Siu, M.J. Stokes, and P.C.W. Fung, "Very-low-frequency anelastic study of $YBa_2Cu_3O_{7-\delta}$ in thermal cycling," to be published.

[129] L. Sun, Y. Wang, H. Shen, and X. Cheng, "Effect of structural instability between 80 and 300 K on superconductivity of $YBa_2Cu_3O_x$," Phys. Rev. B **38**, 5114 (1988).

[130] R. Srinivasan, K.S. Girirajan, V. Ganesan, V. Radhakrishnan, and G.V.S. Rao, "Anomalous variation of the c lattice parameter of a sample of $YBa_2Cu_3O_{7-\delta}$ through the superconducting transition," Phys. Rev. B **38**, 889 (1988).

[131] L.Ya. Kobelev, L.L. Nugaeva, Yu.F. Gorin, Yu.A. Lobanov, and V.B. Zlokazov, "Anomalies of the temperature dependence of the velocity of sound in $YBa_2Cu_3O_7$," Sov. Phys. Solid State **30**, 714 (1988).

[132] L.G. Mamsurova, K.S. Pigalskiy, V.P. Sakun, L.G. Shcherbakova, I.E. Graboy, and A.R. Kaul, "Thermal hysteresis of the elastic modulus and low-temperature local order-disorder phase transitions in $YBa_2Cu_3O_x$ superconductors," JETP Lett. **48**, 217 (1988).

[133] V.G. Baryakhtar, V.N. Varyukhin, O.I. Datsko, A.V. Reznikov, and S.B. Strongin, "Temperature spectrum of internal friction in LaSrCuO and YBaCuO systems," Sov. J. Low Temp. Phys. **14**, 541 (1988).

[134] L.A. Chernozatonskiy, A.I. Golovashkin, O.M. Ivanenko, K.V. Mitsen, L.L. Paltsev, V.I. Pustovoyt, E.F. Tokarev, F.Sh. Khatamov, and V.N. Shorin, "Temperature dependence of the velocity of sound in Y–Ba–Cu–O," Sov. Phys. Solid State **30**,510 (1988).

[135] A.L Gaiduk, S.V. Zherlitsyn, O.R. Prikhodko, V.D. Fil, V.P. seminozhenko, V.F. Nesterenko, and S.A. Pershin, "High-frequency acoustic properties of yttrium ceramics," Sov. J. Low Temp. Phys. **14**, 395 (1988).

[136] A. Hikata, M.J. McKenna, C. Elbaum, R. Kershaw, and A. Wold, "Ultrasonic studies of the relation between two-level-tunneling systems, oxygen content, and superconducting transition temperature in $YBa_2Cu_3O_{7-\delta}$," Phys. Rev. B **40**, 5247 (1989).

[137] D.P. Almond, "Ultrasonic properties of high T_c superconductors," to be published in Proc. Ultrasonics International 89.

[138] A.I. Golovashkin, V.A. Danilov, O.I. Ivanenko, K.V. Mitsen, and I.I. Perepechko, "Acoustic and thermophysical characteristics of a high-temperature superconductor," Sov. Phys. Dokl. **34**, 243 (1989).

[139] G. Cannelli, R. Cantelli, F. Cordero, G. Costa, M. Ferretti, and G.L. Olcese, "An internal friction and frequency study in $YBa_2Cu_3O_{7-x}$," Physica C **153–155**, 298 (1988).

[140] X. Cheng, L. Sun, Y. Wang, H. Shen, and Z. Yu, "Relationship between the phase-transition-like anomalies above T_c and superconductivity in $YBa_2Cu_3O_x$," J. Phys. C: Solid State Phys. **21**, 4603 (1988).

[141] Y. He, S. Lin, B. Zhang, J. Xiang, W. Cui, Y. Li, J. Zhang, C. Lin, J. Li, C. Li, and D. Yin, "An ultrasonic study of energy-gap and granular characteristics of $Y_1Ba_2Cu_3O_{7-y}$ superconducting ceramic," J. Phys. C: Solid State Phys. **21**, L783 (1988).

[142] M. Levy, M.-F. Xu, H.-P. Baum, A. Schenstrom, Y.J. Qian, K.J. Sun, and B. K. Sarma, "Ultrasonic attenuation measurement in high T_c superconductors and heavy Fermion superconductors," in *IEEE 1987 Ultrasonics Symposium* (IEEE, Denver, 1987), p. 1151.

[143] H. Mathias, W. Moulton, H.K. Ng, S.J. Pan, K.K. Pan, L.H. Peirce, L.R. Testardi, and R.J. Kennedy, "Large 'forbidden' change in elastic modulus at the superconducting transition of $Y_1Ba_2Cu_3O_{9-x}$," Phys. Rev. B **36**, 2411 (1987).

[144] H. Mizubayashi, K. Takita, and S. Okuda, "Simultaneous measurements of the anelastic properties and the resistivity in $YBa_2Cu_3O_{7-\delta}$," to be published.

[145] G. Cannelli, R. Cantelli, and F. Cordero, "New anelastic relaxation effect in Y−Ba−Cu−O at low temperature: a Snoek-type peak due to oxygen diffusion," Phys. Rev. B **38**, 7200 (1988).

[146] G. Cannelli, R. Cannelli, F. Cordero, G. A. Costa, M. Ferretti, and G. L. Olcese, "Anelastic relaxation in the high-T_c superconductor $YBa_2Cu_3O_{7-x}$," Phys. Rev. B **36**, 8907 (1987).

[147] G. Cannelli, R. Cantelli, F. Cordero, G.A. Costa, M. Ferretti, and G.L. Olcese, "Phase transformation at 240 K in $YBa_2Cu_3O_{7-x}$ by measurements of elastic energy dissipation and modulus and its possible relation with enhancement of T_c above 100 K," Europhys. Lett. **6**, 271 (1988).

[148] T. Lægreid and K. Fossheim, "Evidence for glasslike dynamic behavior in $YBa_2Cu_3O_{7-x}$ (YBCO) superconductor?" Europhys. Lett. **6**, 81 (1988).

[149] Yu.A. Burenkov, V.I. Ivanov, A.B. Lebedev, B.L. Baskin, B.K. Kardashev, S.P. Nikanorov, Yu.P. Stepanov, V.G. Fleysher, V.N. Varyukhin, O.I. Datsko, and A.V. Reznikov, "Temperature dependences of the absorption of ultrasound and of the Young modulus of superconducting metallic ceramic $YBa_2Cu_3O_{7-x}$," Sov. Phys. Solid State **30**, 1837 (1988).

[150] F. Guillon and J.E. Klemberg-Sapieha, "Intrinsic ultrasonic attenuation in $YBa_2Cu_3O_{7-x}$," Phys. Lett. A **131**, 315 (1988).

[151] B. Kusz and L. Murawski, "The internal friction in superconducting $YBa_2Cu_3O_7$ and semiconducting $YBa_2Cu_3O_6$ ceramics," Solid State Commun. **67**, 435 (1988).

[152] N.D. Patel, P. Sarkar, T. Troczynski, A. Tan, and P.S. Nicholson, "Electrical, mechanical and ultrasonic properties of a sintering-aid modified $YBa_2Cu_3O_x$ high-T_c superconductor," Adv. Ceram. Mater. **2**, 615 (1987).

[153] D.P. Almond, "An ultrasonic study of superconducting and non-superconducting $GdBa_2Cu_3O_{7-x}$," J. Phys. : Cond. Matter. **38**, 6853 (1989).

[154] G. Cannelli, R. Cantelli, and F. Cordero, "Ordering and diffusion of oxygen at low temperature in Y−Ba−Cu−O by measurements of elastic energy dissipation and modulus," Inter. J. Mod. Phys. B **1**, 1157 (1988).

[155] T. Chen, J. Zhang, J. Huang, Y. Chen, M. Yang, X. Xie, T. Li, and L. Xie, "Low and Audio frequency internal friction in high T_c Y−Ba−Cu−O system," Chinese Phys. Lett. **5**, 185 (1988).

[156] I.M. Golev, O.N. Ivanov, I.M. Shushlebin, S.A. Gridnev, and V.E. Miloshenko, "Attenuation of low-frequency sound in Y−Ba−Cu−O metal ceramics," Sov. Phys. Solid State **31**, 120 (1989).

[157] A.G. Ivanov, L.P. Volkova, O.V. Grigut, A.I. Popovich, Yu.F. Revenko, V.M. Svistunov, V.Yu. Tarenkov, L.T. Tsymbal, and A.N. Cherkasov, "Absorption of longitudinal ultrasound in the high-temperature superconductor $Y_{1.2}Ba_{0.8}CuO_{4-y}$," Sov. J. Low Temp. Phys. **14**, 112 (1988).

[158] H. Mizubayashi, K. Takita, and S. Okuda, "Anelastic properties of single-phase $YBa_2Cu_3O_{7-\delta}$," Phys. Rev. B **37**, 9777 (1988).

[159] R.A. Fisher, J.E. Gordon, S. Kim, N.E. Phillips, and A.M. Stacy, "Specific heat of $YBa_2Cu_3O_7$," Physica C **153–155**, 1092 (1988).

[160] Y.S. He, J. Xiang, F.G. Chang, J.C. Zhang, A.S. He, H. Wang, and B.L. Gu, "Anomalous structural changes and elastic properties of bismuth oxide superconductors," Physica C **162−164**, 450 (1989).

[161] H.M. Ledbetter, S.A. Kim, C.E. Violet, and J.D. Thompson, "Low-temperature elastic constants of polycrystalline La_2CuO_4 and $La_{1.85}Sr_{0.15}CuO_4$," Physica C **162−164**, 460 (1989).

[162] D.M. Ginsberg, M.E. Reeves, S.E. Stupp, T.A. Friedmann, F. Slakey, and M.V. Klein, "Specific heat of polycrystalline $YBa_2Cu_3O_{7-x}$ in a magnetic field," Physica C **162–164**, 486 (1989).

[163] R.A. Fisher, S. Kim, Y. Wu, N.E. Phillips, H.M. Ledbetter, and K. Togano, "Specific heat in the high-T_c superconductor $(Bi_{1.66}Pb_{0.34})Ca_2Sr_2Cu_3O_{10}$," Physica C **162–164**, 502 (1989).

[164] R. Jin, F. Shi, Q. Ran, N. Shi, Z. Shi, S. Zhou, and B. Jin, "The specific heat of single-phase $(Bi,Pb)_2Sr_2Ca_2Cu_3O_{10+y}$ superconductor," M^2S-HTSC Conference (Stanford, July 1989).

[165] A. Junod, D. Eckert, T. Graf, G. Triscone, and J. Müller, "$YBa_2Cu_3O_{7-\delta}$: improvement of the specific heat behavior at low temperatures and near T_c," Physica C **162–164**, 482 (1989).

[166] G.K. White, S.J. Collocott, R. Driver, R.B. Roberts, and A.M. Stewart, "Thermal properties of high-T_c superconductors," J. Phys. C: Solid State Phys. **21**, L631 (1988).

[167] V. Müller, K. de Groot, D. Maurer, C. Roth, and K.H. Rieder, "Ultrasonic experiments on the high-T_c-superconductor $Y_{2-x}Ba_xCuO_{4-\delta}$," Physica **148B**, 296 (1987).

[168] V.V. Zoninashvili and I.A. Naskidashvili, "Elastic relaxation in the superconducting ceramic $Y_1Ba_2Cu_3O_{7-\delta}$," Sov. Tech. Phys. Lett. **14**, 904 (1988).

[169] P.L. Gammel, L.F. Schneemeyer, J.V. Waszczak, and D.J. Bishop, "Evidence from mechanical measurements for flux-lattice melting in single-crystal $YBa_2Cu_3O_7$ and $Bi_{2.2}Sr_2Ca_{0.8}Cu_2O_8$," Phys. Rev. B **61**, 1666 (1988).

[170] P. Baumgart, S. Blumenröder, A. Erle, B. Hillebrands, G. Güntherodt, and H. Schmidt, "Sound velocities of $YBa_2Cu_3O_{7-\delta}$ single crystal measured by Brillouin spectroscopy," Solid State Commun. **69**, 1135 (1989).

[171] P. Baumgart, S. Blumenröder, A. Erle, B. Hillebrands, P. Splittgerber, G. Grüntherodt, and H. Schmidt, "Sound velocities of $YBa_2Cu_3O_{7-\delta}$

and $Bi_2Sr_2CaCu_2O_x$ single crystals measured by Brillouin spectroscopy," Physica C **162–164**, 1073 (1989).

[172] W. Reichardt, L. Pintschovius, B. Hennion, and F. Collin, "Inelastic neutron scattering study of $YBa_2Cu_3O_{7-x}$," Supercond. Sci. Technol. **1**, 173 (1988).

[173] I.V. Aleksandrov, A.F. Goncharov, and S.M. Stishov, "Equation of state and compressibility of single crystals of the high-temperature superconductor $YBa_2Cu_3O_x$ at pressures up to 20 GPa," JEPT Lett. **47**, 428 (1988).

[174] H.M. Ledbetter and Ming Lei, "Is $Y_1Ba_2Cu_3O_7$ stiff or soft?" J. Mater. Res. **5**, 241 (1990).

[175] Y.P. Varshni, "Temperature dependence of the elastic constants," Phys. Rev. **2**, 3952 (1970).

[176] T. Datta, H.M. Ledbetter, C.E. Violet, C. Almasan, and J. Estrada, "Reentrant softening in perovskitelike superconductors," Phys. Rev. B **37**, 7502 (1988).

[177] V. Müller, D. Maurer, C. Roth, C. Hucho, D. Winau, and K. de Groot, "Ultrasonic hysteresis effects and the formation of twin domains in high-T_c superconductors," Physica C **153–155**, 280 (1988).

[178] D.P. Almond, G.A. Saunders, and E.F. Lambson, "Ultrasonic evidence indicating $YBa_2Cu_3O_{7-x}$ to be a pseudoplastic material," Supercond. Sci. Technol. **1**, 163 (1988).

[179] Y. Nakazawa, M. Ishikawa, T. Takabatake, K. Koga, and K. Terakura, "Characterization of metamorphic phases of $Ba_2YCu_3O_{9-\delta}$," Jpn. J. Appl. Phys. **26**, L796 (1987).

[180] B. Bridge and R. Round,"Computation of the bulk modulus of the high temperature ceramic superconductor $YBa_2Cu_3O_{7-x}$ from unit cell data," J Mater. Sci. Lett.7, 63 (1988).

[181] S. Valkealahti and D.O. Welch, "Theoretical studies of structural properties of the high-T_c oxide superconductor $YBa_2Cu_3O_{7-x}$," M^2S-HTSC Conference (Stanford, July 1989).

[182] I.M. Vitebskii, N.M. Lavrinenko, V.P. Seminozhenko, and V.L. Sobolev, "Theory of elastic and acoustic properties of polydomain ferroelastics of the La_2CuO_4 and $YBa_2Cu_3O_{7-x}$ type," M^2S-HTSC Conference (Stanford, July 1989).

[183] A.J. Millis and K.M. Rabe, "Superconductivity and lattice distortions in high-T_c superconductors," Phys. Rev. B **38**, 8908 (1988).

[184] D.J. Bishop, P.L. Gammel, A.P. Ramirez, R.J. Cava, B. Batlogg, and E.A. Rietman, "Ultrasound studies of the high-T_c superconductor $La_{1.85}Sr_{0.15}CuO_4$," Phys. Rev. B **35**, 8788 (1987).

[185] R. Yoshizaki, T. Hikata, T. Han, T. Iwazumi, H. Sawada, T. Sakudo, T. Suzuki, and E. Matsuura, "Acoustic property measurement of the oxide superconductor $(La_{1-x}Sr_x)_2CuO_4$ by the sphere resonance method," Jpn. J. Appl. Phys. Suppl. **26–3**, 1129 (1987).

[186] A. Al-Kheffaji, J. Freestone, D.P. Almond, G.A. Saunders, and Jing Wang, "A comparison of the ultrasonic evidence for mode-softening in $La_{1.8}Sr_{0.2}CuO_4$ and the electron doped superconductor $Nd_{1.85}Ce_{0.15}CuO_{4-y}$," J. Phys. : Cond. Matter, to be published.

[187] P. Esquinazi, J. Luzuriaga, C. Durán, D.A. Esparza, and C. D'Ovidio, "Anomalies in the internal friction and sound velocity in the high-temperature superconductor $La_{1.8}Sr_{0.2}CuO_4$," Phys. Rev. B **36**, 2316 (1987).

[188] M.N. Regueiro, P. Esquinazi, M.A. Izbizky, C. Durán, D. Castello, and J. Luzuriaga, "Tunneling systems in high temperature superconductors," Ann. Phys. Fr. **13**, 401 (1988).

[189] L.C. Bourne, A. Zettl, K.C. Chang, M.L. Cohen, A.M. Stacy, and W.K. Ham, "Elasticity studies of $La_{2-x}Sr_xCuO_4$," Phys. Rev. B **35**, 8785 (1987).

[190] X.-D. Xiang, J.W. Brill, L.E. Delong, L.C. Bourne, A. Zettl, J.C. Jones, and L.A. Rice, "Elastic properties of polycrystalline $La_{2-x}Sr_xCuO_4$," Solid State Commun. **65**, 1073 (1988).

[191] W.-K. Lee, M. Lew, and A.S. Nowick, "Elastic softening and internal friction in $La_{2-x}Sr_xCuO_4$," submitted to Phys. Rev. B (1989).

[192] V.N. Varyukhin, A.V. Reznikov, O.V. Grigut, O.I. Datsko, L.A. Zilberman, and Yu.F. Revenko, "Acoustic attenuation in the $La_{1.8}Sr_{0.2}CuO_4$ system," JETP Lett. **46**, S132 (1987).

[193] A.L. Gaiduk, S.V. Zherlitsyn, A.S. Panfilov, V.M. Puzikov, A.M. Stepanenko, V.D. Fil, and A.S. Chernyi, "Anomalous behavior of the elastic modulus in $La_{1.8}Sr_{0.2}CuO_4$," Sov. J. Low Temp. Phys. **13**, 370 (1987).

[194] Y. Horie, T. Fukami, and S. Mase, "Ultrasonic studies of the high T_c superconductor $(La_{1-x}Sr_x)_2CuO_{4-\delta}$," Solid State Commun. **63**, 653 (1987).

[195] A.M. Burkhanov, V.V. Gudkov, I.V. Zhevstovskikh, V.L. Kozhevnikov, V.Ye. Naysh, S.M. Podgornykh, V.Ye. Startsev, A.V. Tkach, V.V. Ustinov, V.A. Fotiyev, S.M. Cheshnitskiy, and S.V. Yartsev, "Elastic properties and thermal expansion of $La_{1.83}Sr_{0.17}CuO_4$," Phys. Met. Metall. **64**, 176 (1987).

[196] V.G. Baryakhtar, V.M. Pan, V.F. Taborov, V.F. Tarasov, N.V. Shevchuk, O.I. Shulishova, and A.I. Shcherbak, "Temperature dependence of the ultrasound velocity in a lanthanum cermet," Sov. J. Low Temp. Phys. **13**, 485 (1987).

[197] J. Hu, S. Zhang, Q. Zhang, W. Cai, T. Deng, L. Zhang, Y. He, and X. Jiong, "Ultrasonic attenuation and velocity in BiSrCaCuO high T_c superconductor," Physica C **162–164**, 444 (1989).

[198] Y. Wang, J. Wu, J. Zhu, H. Shen, Y. Yan, and Z. Zhao, "Ultrasonic study on structural instability of $Bi_2Sr_2Ca_1Cu_2O_8$ single crystal," Physica C **162–164**, 454 (1989).

[199] X.D. Xiang, M. Chung, J.W. Brill, S. Hoen, P. Pinsukanjana, and A. Zettl, "Elastic properties of single crystal $Bi_2Sr_2CaCu_2O_8$," Solid State Commun. **69**, 833 (1989).

[200] Y. Wang, J. Wu, J. Zhu, H. Shen, J. Zhang, Y. Yan, and Z. Zhao, "Ultrasonic study on anisotropic elasticity of $Bi_2Sr_2Ca_1Cu_2O_8$ single crystal," submitted to Phys. Rev. B (1989).

[201] V. Plechácek and J. Dominec, "Sound velocities in single-phase 2223 Bi,Pb−Sr−Ca−Cu−O polycrystalline superconductor," submitted to Solid State Commun. (1989).

[202] S. Lin, Y. He, C. Wei, and Z. Shen, "Elastic constants of single-phase $Bi_2Sr_2CaCu_2O_{8+y}$ superconductor," Supercond. Sci. Technol. **2**, 145 (1989).

[203] K.J. Sun, W.P. Winfree, M.F. Xu, M. Levy, Bimal K. Sarma, A.K. Singh, M.S. Osofsky, and V.M. Le Tourneau, "Ultrasonic attenuation anomaly of Tl−Ca−Ba−Cu−O at superconducting transition," Physica C **162−164**,446 (1989).

[204] Y. Wang, X. Chen, H. Shen, and L. Sun, "Relationship between lattice instability and superconductivity in high T_c oxide superconductors," Physica C **162−164**, 456 (1989).

[205] D.O. Pederson, A.El Ali, Z.Z. Sheng, and A.M. Hermann, "Ultrasonic attenuation measurements on thallium-based high-temperature superconductors," Phys. Rev. B **40**, 7313 (1989).

[206] R. Moret, Alan I. Goldman, and A. Moodenbaugh, "Compressibility of the high-T_c superconductor $La_{1.7}Ba_{0.3}CuO_{4-y}$," Phys. Rev. B **37**, 7867 (1988).

[207] H. Takahashi, C. Murayama, S. Yomo, N. Mori, K. Kishio, K. Kitazawa, and K. Fueki, "Pressure effect on the lattice constant and compressibility of a superconductor $(La_{0.9}Sr_{0.1})_2CuO_{4-y}$," Jpn. J. Appl. Phys. **26**, L504 (1987).

[208] H. Takahashi, C. Murayama, S. Yomo, N. Möri, W. Ustumi, and T. Yagi, "High-pressure x-ray study on $(La_{1-x}A_x)_aCu_bO_c$ system," Jpn. J. Appl. Phys. Suppl. **26−3**, 1109 (1987).

[209] H.M. Ledbetter, N.V. Frederick, and M. W. Austin, "Elastic-constant variability in stainless-steel 304," J. Appl. Phys. **51**, 305 (1980).

[210] R. Hearmon, "The elastic constants of polycrystalline aggregates," in *Physics of the Solid State* (Academic, New York, 1969). p. 401.

[211] H.M. Ledbetter and S.K. Datta, "Effective wave speeds in an SiC-particle-reinforced Al composite," J. Acoust. Soc. Amer. **79**, 239 (1986).

[212] R.H. Fowler and E.A. Guggenheim, *Statistical Thermodynamics* (Cambridge University Press, London, 1960), p. 140.

[213] S.E. Inderhees, M.B. Salamon, T.A. Friedmann, and D.M. Ginsberg, "Measurement of the specific-heat anomaly at the superconducting transition of $YBa_2Cu_3O_{7-\delta}$," Phys. Rev. B **36**, 2401 (1987).

[214] H.M. Ledbetter, "Grüneisen parameter of $Y_1Ba_2Cu_3O_7$," Physica C **159**, 488 (1989).

[215] F.H. Herbstein, "Methods of measuring Debye temperature and comparison of results for some cubic crystals," Adv. Phys. **10**, 313 (1961).

[216] J.L. Feldman, "The relation between Θ(elastic) and Θ(calorimetric) near $T = 0$ K," Proc. Phys. Soc. **84**, 361 (1964).

[217] R.A. Fisher, J.E. Gorden, and N.E. Phillips, "Specific heat of the high-T_c oxide superconductors," J. Supercond. **1**, 231 (1988).

[218] F.C. Brown, *The Physics of Solids* (Benjamin, New York, 1967), p. 94.

[219] P.P. Ewald, "The Calculation of optical and electrostatic lattice potentials," Ann. Phys. **64**, 253 (1921).

[220] W. van Gool and A.G. Piken, "Lattice self-potentials and Madelung constants for some compounds," J. Mater. Sci. **4**, 95 (1969).

[221] M. Tosi, "Cohesion of ionic solids in the Born model," in *Solid State Physics*, eds. F. Seitz and D. Turnbull (Academic, New York, 1964), Vol. **16**, p. 54.

[222] E.R. Naimon, "Elastic constants of the perovskite $RbMnF_3$ using a Born model," Phys. Rev. B **9**, 737 (1974).

[223] E. Iguchi and Y. Yonezawa, "Madelung potentials in $YBa_2Cu_3O_x$ (x=7 and 8)," Jpn. J. Appl. Phys. **26**, L1492 (1987).

[224] W.I.F. David, W.T.A. Harrison, J.M.F. Gunn, O. Moze, A.K. Soper, P. Day, J.D. Jorgensen, D.G. Hinks, M.A. Beno, L. Soderholm, D.W. Capone II, I.K. Schuller, C.U. Seger, K. Zhang, and J.D. Grace, "Structure and crystal chemistry of the high-T_c superconductor $YBa_2Cu_3O_{7-x}$," Nature **327**, 310 (1987).

[225] D.L. Anderson and O.L. Anderson, "The Bulk modulus-volume relationship for oxides," J. Geophys. Res. **75**, 3494 (1970).

[226] R. Baetzold, "Atomistic simulation of ionic and electronic defects in $YBa_2Cu_3O_7$," Phys. Rev. B **38**, 11304 (1988).

[227] W.E. Peckett, "Electronic structure of the high-T_c oxide superconductors," Rev. Mod. Phys. **61**, 433 (1989).

[228] W.L. McMillan, "Transition temperature of strong-coupled superconductors," Phys. Rev. **167**, 331 (1968).

[229] P.B. Allen and R.C. Dynes, "Transition temperature of strong-coupled superconductors reanalyzed," Phys. Rev. B **12**, 905 (1975).

[230] V.Z. Kresin, "On the critical temperature for any strength of the electron–phonon coupling," Phys. Lett. A **122**, 434 (1987).

[231] J. Rammer, "Strong-coupling calculation of the lower critical field high-T_c superconductors," Phys. Rev. B **36**, 5665 (1987).

[232] Z. Schlesinger, R.L. Greene, J.G. Bednorz, and K.A. Müller, "Far-infrared measurement of the energy gap of $La_{1.8}Sr_{0.1}CuO_4$," Phys. Rev. B **35**, 5334 (1987).

[233] V.Z. Kresin and S.A. Wolf, "A method for evaluating the electron–phonon coupling in cuprates from heat capacity measurements," Physica C **158**, 76 (1989).

[234] R. Zeyer and G. Zwicknagl, "Phonon self-energy effects due to superconductivity: Evidence for the strong-coupling limit in $YBa_2Cu_3O_{7-\delta}$," Solid State Commun. **66**, 617 (1988).

[235] N.F. Wright and W.H. Butler, "Ionic models for $YBa_2Cu_3O_7$ and $YBa_2Cu_3O_6$," in *High-Temperature Superconductors II* (MRS, Pittsbutgh, 1988) p. 25.

[236] W. Kress, U. Schrödrer, J. Prade, A.D. Kulkarni, and F.W. de Wette, "Lattice dynamics of $YBa_2Cu_3O_{7-x}$," Physica C **153–155**, 221 (1988).

[237] R.E. Cohen, W.E. Pickett, H. Krakauer, and L.L. Boyer, "Application of ionic models to the high-temperature superconductor La_2CuO_4," Physica C **150**, 61 (1988).

[238] J. Kondo, Y. Asai, and S. Nagai, "The Madelung energy in copper-oxide-based ceramics," J. Phys. Soc. Jpn. **57**, 4334 (1988).

[239] V. Müller, "Possible origin of high-T_c superconductivity in (1–2–3) oxides," Solid State Commun. **67**, 805 (1988).

[240] F. Beech, S. Miraglia, A. Santoro, and R.S. Roth, "Neutron study of the crystal structure and vacancy distribution in the superconductor $Ba_2YCu_3O_{9-\delta}$," Phys. Rev. B **35**, 8778 (1987).

[241] D. Shoenberg, *Superconductivity* (Cambridge U.P., Cambridge, 1952), pp. 73–77.

[242] I.V. Berman, N.B. Brandt, I.L. Romashkina, V.I. Sidorov, and C.Y. Han, "The effect of a high pressure up to 210 kbar upon the superconductivity of monocrystalline and ceramic specimens of $YBa_2Cu_3O_{7-y}$," in *High Temperature Superconductivity from Russia* (World Scientific, Singapore, 1989), p. 250.

[243] R. Griessen, "Pressure dependence of high-T_c superconductors," Phys. Rev. B **36**, 5284 (1987). Also see the references therein.

[244] J.L. Tallon and J. Lusk, "High-pressure studies on the 90 K superconductors $Y_2Ba_4Cu_4O_15$ and $(Y/Ca)Ba_2Cu_4O_8$," Physica C **167**, 236 (1990).

[245] M.F. Crommie, A.Y. Liu, A. Zettl, M.L. Cohen, P. Parilla, M.F. Hundley, W.N. Creager, S. Hoen, and M.S. Sherwin, "c-axis stress dependence of normal and superconducting state properties of $YBa_2Cu_3O_7$," Phys. Rev. B **39**, 4231 (1989).

[246] U. Koch, J. Witting, and B. Gegenheimer, "Toward the true stress dependence of T_c for $YBa_2Cu_3O_{6.9}$," Physica C **162–164**, 739 (1989).

[247] C. Meingast, B. Blank, H. Bürkle, B. Obst, T. Wolf, and H. Wühl, "Anisotropic pressure dependence of T_c in single crystal $YBa_2Cu_3O_7$ via thermal expansion," preprint (1990).

[248] Y. Ohta, T. Tohyama, and S. Maekawa, "Apex oxygen and critical temperature in Cu-oxide superconductors: Universal correlation with the stability of local singlet," submitted to Phys. Rev. B (1990).

[249] R.J. Cava, A.W. Hewat, E.A. Hewat, B. Batlogg, M. Marezio, K.M. Rabe, J.J. Krajewski, W.F. Peck Jr, and L.W. Rupp Jr, "Structural anomalies, oxygen ordering and superconductivity in oxygen deficient $Ba_2YCu_3O_x$," Physica C **165**, 419 (1990).

Appendix A

Measured Elastic Constants of Polycrystal YBCO

Table A.1: Measured elastic constants of polycrystal YBCO.

First author	Temp. (K)	B (GPa)	E (GPa)	G (GPa)	ν
Alford [85]	300		214.00		
Al-Kheffaji [83]	295	42.40	78.00	32.70	0.194
Al-Kheffaji [83]	295	56.40	116.00	50.10	0.157
Al-Kheffaji [83][a]	295	68.50	135.00	57.40	0.149
Almond [53]	205	46.30	88.50	37.40	0.182
Block [52]	295	196.00	235.00		
Bridge [88][a]	300	50.20	99.80	42.70	0.169
Chang [90][a]	300		226.00	87.00	0.300
Dietrich [80]	300	170.00			
Fietz [81]	300	180.00			
Glazkov [89]	300	175.40			
Glazkov [89]	300	112.40			
Kim [78]	220	26.90			0.194
Jaya [82]	295	92.86			
Ledbetter [51][a]	295	72.20	90.80	35.20	0.290
Ledbetter [51][a]	295	56.10	101.80	42.50	0.198
Lee [70][a]	295		145.10	59.00	
Round [86]	300	38.00	64.00	26.00	0.220
Salama [91]	300		117.00	48.00	
Salomons [79]	300	56.30			
Severin [87]	300		112.00		0.250
Staines [71][a]	295		118.00		
Tallon [72]	295	115.00	104.00	39.00	0.350
Wolf [67]	220	38.80			0.190
Yoshimoto [77]	295	55.08	84.01	33.72	0.246

[a] Corrected to void-free state.

BL-114A
(5-90)

U.S. DEPARTMENT OF COMMERCE
NATIONAL INSTITUTE OF STANDARDS AND TECHNOLOGY

BIBLIOGRAPHIC DATA SHEET

1. PUBLICATION OR REPORT NUMBER
NISTIR 3980

2. PERFORMING ORGANIZATION REPORT NUMBER

3. PUBLICATION DATE
August 1991

4. TITLE AND SUBTITLE

OXIDES AND OXIDE SUPERCONDUCTORS:
ELASTIC AND RELATED PROPERTIES

5. AUTHOR(S)

Ming Lei and Hassel Ledbetter

6. PERFORMING ORGANIZATION (IF JOINT OR OTHER THAN NIST, SEE INSTRUCTIONS)

U.S. DEPARTMENT OF COMMERCE
NATIONAL INSTITUTE OF STANDARDS AND TECHNOLOGY
BOULDER, COLORADO 80303-3328

7. CONTRACT/GRANT NUMBER

8. TYPE OF REPORT AND PERIOD COVERED

9. SPONSORING ORGANIZATION NAME AND COMPLETE ADDRESS (STREET, CITY, STATE, ZIP)

10. SUPPLEMENTARY NOTES

11. Using both measurements and modeling, the elastic and related properties of some oxides and oxide superconductors were studied. The polycrystal elastic constants were measured using a MHz-frequency pulse-echo method between 295 and 4 K and corrected to the void-free state by using a model for a composite material containing spherical particles. The elastic moduli of the high-T_c superconductor $Y_1Ba_2Cu_3O_7$ (YBCO) were compared with that of oxides, especially the perovskites $BaTiO_3$ and $SrTiO_3$, which are crystal-structure building blocks for the YBCO superconductor. The bulk moduli were also calculated using a Born ionic model with two energy terms: electrostatic (Madelung) and ion-core-repulsion. The calculated bulk modulus of YBCO, 98 GPa, agrees well with measurement, 101 GPa. Based on monocrystal measurements combined with analysis–theory, elastic stiffnesses C_{ij} for orthorhombic YBCO were estimated. The bulk modulus obtained from the estimated C_{ij} by the Voigt–Reuss–Hill averaging method agrees with the monocrystal measurement. From the measured polycrystalline elastic constants, the Debye characteristic temperatures, Θ_D, were calculated. For YBCO, $\Theta_D^0 = 437$ K. The electron–phonon parameters, λ, were estimated from T_c and Θ_D^0 using Kresin's model, which is valid for all values of λ. For YBCO, $\lambda = 2.24$. By calculating the Madelung energy, two further features were studied: the valence of copper and the electron hole distribution. The results show that the hole prefers the CuO_2 plane at the oxygen sites. All the results are consistent with the assumption that all copper ions have valences near +2. Using a relationship between T_c and ΔV_A, the difference in Madelung site potentials for a hole at the apical and planar oxygens, the pressure derivative and stress and strain derivatives of T_c were calculated. The results show that T_c increases with decreasing a-axis, increasing b-axis, and decreasing c-axis.

12. KEY WORDS (6 TO 12 ENTRIES; ALPHABETICAL ORDER; CAPITALIZE ONLY PROPER NAMES; AND SEPARATE KEY WORDS BY SEMICOLONS)

Born model; bulk modulus; Debye temperature; elastic constants; electron-phonon parameter; Kresin model; oxides; pressure derivative; superconductors; $Y_1Ba_2Cu_3O_7$.

13. AVAILABILITY

[X] UNLIMITED

[ ] FOR OFFICIAL DISTRIBUTION. DO NOT RELEASE TO NATIONAL TECHNICAL INFORMATION SERVICE (NTIS).

[ ] ORDER FROM SUPERINTENDENT OF DOCUMENTS, U.S. GOVERNMENT PRINTING OFFICE, WASHINGTON, DC 20402.

[X] ORDER FROM NATIONAL TECHNICAL INFORMATION SERVICE (NTIS), SPRINGFIELD, VA 22161.

14. NUMBER OF PRINTED PAGES
100

15. PRICE
A05

ELECTRONIC FORM